Review Article

Nano Research
2021, 14(11): 3724–3743

ISSN 1998-0124 CN 11-5974/O4
https://doi.org/10.1007/s12274-021-3336-9

Advances in green synthesis and applications of graphene

Qi Yu[1,2] (✉), Jianchao Jiang[1], Liyun Jiang[1], Qingqing Yang[1], and Ning Yan[2]

[1] *Shaanxi Key Laboratory of Catalysis, School of Materials Science and Engineering, Shaanxi University of Technology, Hanzhong 723001, China*
2 Department of Chemical and Biomolecular Engineering, National University of Singapore, Singapore 117585, Singapore

© Tsinghua University Press and Springer-Verlag GmbH Germany, part of Springer Nature 2021
Received: 17 December 2020 / **Revised:** 15 January 2021 / **Accepted:** 18 January 2021

ABSTRACT

Green synthesis has grabbed appreciable attention to eliminate the negative effects associated with various chemical processes. Due to the unparalleled electrical, mechanical, thermal and excellent physical properties, graphene, as the thinnest two-dimensional material with high surface area, has the unfathomable potential in the domain of green chemistry in terms of both synthesis and application. In this regard, we present an overview of the research progresses on the greener synthesis of graphene, including micromechanical exfoliation, chemical reduction of graphene oxide (GO), chemical vapor synthesis and popping of GO. Meanwhile, various applications of graphene pertinent to sustainable developments, such as energy storage, catalysis, electrochemistry, fuel cell, supercapacitor and biomedicine have also been highlighted.

KEYWORDS

green chemistry, graphene, synthesis, catalysis, supercapacitor

1 Introduction

The application of green chemistry has been one of the most impressive research fields to solve the problem of reducing the negative effects on society and environment in the reaction process through chemical strategies, including reactants, reaction environment, reaction products and additives used as catalysis in the reaction process. In 1998, Anastas et al. put forward 12 principles based on the perspective of green chemistry [1]. It is committed to meet the requirements of improving the yield and benefit, as well as reducing the generation of waste and harmful substances, so as to meet the requirements of safety, economy and environmental friendliness.

Graphene, which consists of hexagonal lattice of carbon atoms and sp^2 hybrid orbitals [2, 3], has excellent properties in the electrical, optical, mechanical and thermal fields [4–7], which exhibits high carrier mobility (200,000 $cm^2 \cdot V^{-1} \cdot s^{-1}$) [8], super strength (125 GPa) [9], large specific surface area (2,630 $m^2 \cdot g^{-1}$) [10], high Young's modulus (~ 1,100 GPa) [9], as well as typical bipolar electric field effect and quantum Hall effect of charge carriers [11, 12]. There are many existing research technologies on the preparation, including chemical vapor deposition (CVD) [13–15], epitaxial growth [16], arc discharge [17], chemical embedding [18], and thermal/chemical reduction of GO (Table 1)

Table1 The list of various of synthesis and properties of graphene

Method	Thickness	Lateral	Advantage	Disadvantage
Micromechanical exfoliation [5]	Few layers	μm to cm	Large size and unmodified graphene sheets	Very small scale production
Plasma enhanced chemical vapor deposition [10]	Carbon nanowalls	size of 50–150 nm long and < 10 nm wide	Large growth、less defective and a high degree of crystallinity	High economic cost and insufficient technical maturity
Chemical vapor deposition [11]	Single and few layers	~ 20 μm	A large fraction and features are well controlled	Very small scale production
Epitaxial growth [12]	Single and few layers	> 100 μm	Very large area of pure graphene	Uneven thickness, unstable electronic performance
Arc discharge [13]	2–4 layers	$10–40 \times 10^3$ nm^2	Pure graphene and few layers	High environmental requirements and low production
Chemical embedding [14]	few-layer and single-layer	μm to cm	Good electrical properties and pure graphene	Low production, difficult to control the number of layers
Thermal/chemical reduction of graphene oxide [15, 16]	Single and few layers	μm to cm	Increased conductivity, adjustable performance and reduction	Low yield, limited reductant, uncertain reaction steps and time

Address correspondence to kukukoko2004@163.com

[19, 20]. Based on the above methods, green and efficient industrial production of graphene still faces great challenges. The route of preparing graphene by chemical reduction method has broad application prospect, which has been used for mass production [21, 22]. In general, the preparation of graphene by reducing GO requires strong reductants. The traditional methods are usually by hydrazine or derivatives, however, the strong reductants will produce unstable factors in conventional production with certain impact on the environment [23]. In recent years, green synthesis and applications of graphene have been continuously developed. Meanwhile, low-cost and high-efficiency synthetic route are also the basic principle to promote the application of graphene.

Graphene has many excellent performances, these characteristics have attracted great attentions in the fields of chemistry, physics and materials (Fig. 1). Especially the application prospects in capacitors, electrode materials, catalysis and sensors.

In this review, we will discuss graphene synthesis and application based on the concept of green chemistry. Synthetic methods have been systematically summarized from traditional to innovative categories. It also involves different methods on the performance of the final synthesized graphene. Meanwhile, we are focused on the application of graphene with the concept of green and sustainable, which can be applied to the fields of new energy and catalysis.

2 Green synthesis of graphene

In recent years, it is obvious that the chemical reduction oxidation method of graphene has the prospect of industrial mass production [24, 25]. However, considering that hydrazine or derivatives are mainly used in experiments and production processes, which will cause harmful effects on the environment. Obviously, how to synthesize graphene in a green, safe and efficient way is the factor that determines whether graphene can be full play to potential. Above all, the green synthesis methods such as the micromechanical exfoliation technology [1], chemical reduction method and CVD have been developed [17, 19, 26, 27].

2.1 Greener synthetic protocol

In order to find an innovative route to prepare environmentally friendly graphene, the strategy of "green chemistry" can't be ignored in the synthesis. As a collaborative system, "twelve principles" provide a new reform idea for the development of graphene. The synthesis path, reaction materials and power consumption are "green" designed [28, 29]. Recently, the issue of renewable has become a research hotspot, including looking for green, economic and efficient biomass reducing agent to prepare reduced graphene oxide (RGO) [30]. Meanwhile, the utilization of raw materials and the minimization of waste production are realized, such as graphene can be used in fuel cells with excellent performance, which makes it feasible in environment and economy [31, 32].

2.1.1 *Micromechanical exfoliation*

In 2004, Geim and co-workers firstly used micromechanical exfoliation to obtain graphene from graphite. This technology is also called transparent tape technology [5]. Micromechanical exfoliation is the simplest and lowest cost method for preparing graphene with high yield. The method mainly uses transparent adhesive tape to separate graphite layers. Interlayer graphene is combined by van der Waals force. The weak binding force makes the mechanical stripping feasible [33]. There are two methods to obtain graphene by mechanical peeling: adding force and lateral force. One is the transparent adhesive tape technology, in which a normal force of van der Waals force is applied to peel off between graphite layers. The other is to apply lateral force to promote the mutual displacement between layers, so as to peel off the graphite. However, this route is not feasible for obtaining ideal area (Figs. 2(a) and 2(b)) [34].

Preparation of high-quality graphene from mechanically exfoliated graphite is considered as a first choice. The advantages are not only simple source of materials with low cost, but also high quality that provides a feasible way to expand the synthesis path of graphene [35]. However, there is also some shortcoming in the micromechanical exfoliation method, which leads to the limitation of industrial production. Due to process factors, the yield is greatly limited. At the same time, the mobility of carriers may be limited due to the existence of substrate. Fragmentation effect is still not feasible for the large-area production. As a result, this method greatly limited in the capacity of large-scale production [36, 37]. Fu et al. prepared high-quality graphene using re-expansion and stripping of graphite interlayer compounds (Fig. 2(c)).

Micromechanical stripping technology can provide more ideal strategy for the production of high-quality microstructure

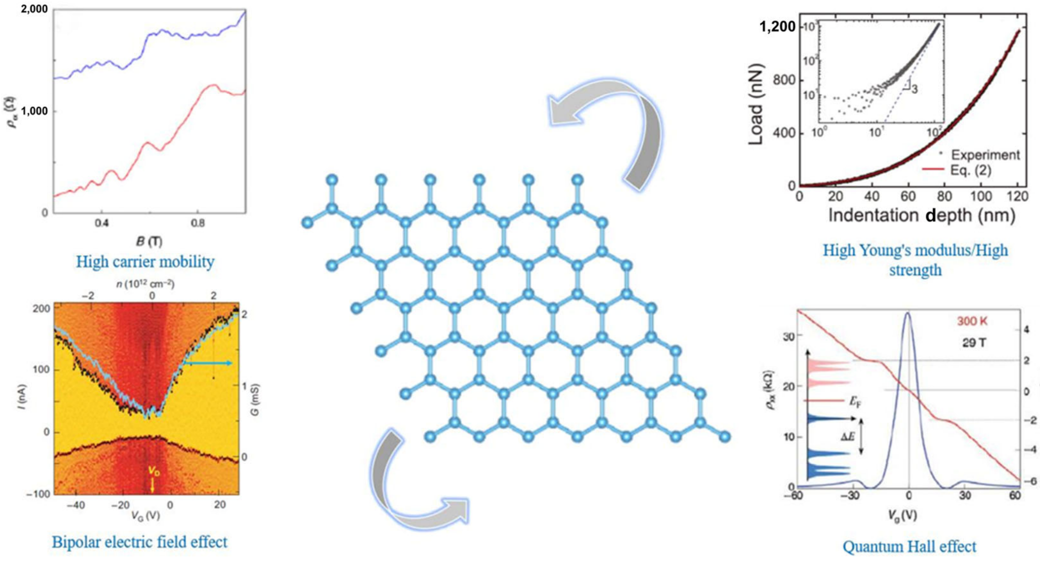

Figure 1 The main characteristics and properties of graphene.

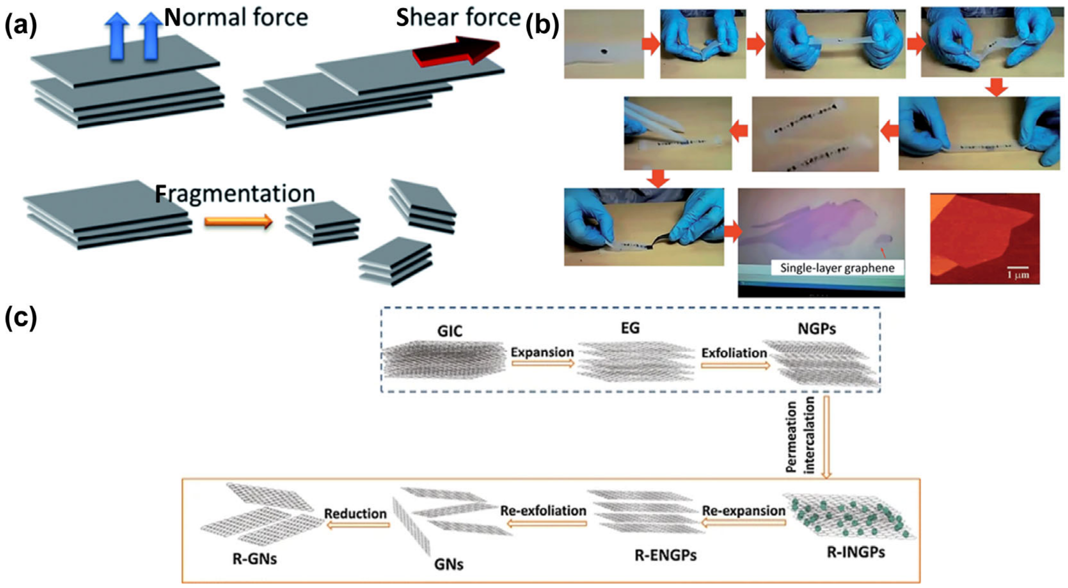

Figure 2 (a) The method of mechanical stripping graphite to fragment graphene. (b) Preparation of highly ordered pyrolytic graphite by transparent tape method. Reproduced with permission from Ref. [34], © The Royal Society of Chemistry 2015. (c) The synthesis path of reduced graphene sheets. Reproduced with permission from Ref. [37], © Springer Science+Business Media New York 2014.

graphene with precise control, including the factors of size, defects and layers.

2.1.2 *Chemical reduction of graphene oxide*

Chemical reduction of GO is a high selectivity synthesis method with low-cost and high-yield [38, 39]. There are two types of synthetic methods, bottom-up and top-down. Bottom-up is a kind of graphene continuously constructed from the original state. While top-down is a method of continuously obtaining graphene through graphite.

GO is an ideal intermediate substance from graphite to graphene. The oxidation treatment can increase the spacing, thus contributing to the exfoliation of graphene [40]. As early as 1859, Brody et al. obtained GO for the first time through experimental preparation. Since then, this method has been continuously improved, high carbon-oxygen ratio GO substitute have been explored [41, 42].

The chemical reduction method requires oxidizing graphite with strong acid or oxidizing agents [43, 44]. There are many choices of reducing agents. Pumera et al. provided a method to divide the reducing agents into two types, which were called the “well-supported” mechanism and “proposed” mechanism. The reducing agents classified include traditional synthetic chemistry reacting with specific oxygen-containing functional groups, since this type of reducing agent has specific functions and reactions. This type of reducing agent does not react against specific oxygen-containing functional groups. Graphite can be transited to graphene through the chemical reduction process from graphite to graphene requires the transition of GO (Fig. 3) [45].

The researches of reducing agent in chemical reduction are mainly with the advantages of high yield of reducing agent, no pollution to the environment, easy removal after reaction and avoidance of products. The existing comprehensive types of reducing agents are as follows. With the “well-supported” mechanism such as borohydride [46, 47], aluminum hydride [48], hydrohalic acid [49], sulfur-containing reducing agents (thiourea dioxide, etc.) [50]. The reducing agents in the classification with “proposed” mechanism are nitrogen-containing reductant (hydrazine, urea, etc.) [51, 52], reductant (alcohol, sugar, gallic acid, etc.) [53, 54], sulfur-containing reducing agents (sulfur-containing compounds, sodium bisulfite, etc.) [55, 56], metal-acid [57, 58], metal-base [59–61], amino acids (glycine, lysine, etc.) [62, 63], plant extracts [64, 65], microorganisms [66], proteins and hormones [67, 68].

In view of the low cost of chemical reduction and the great

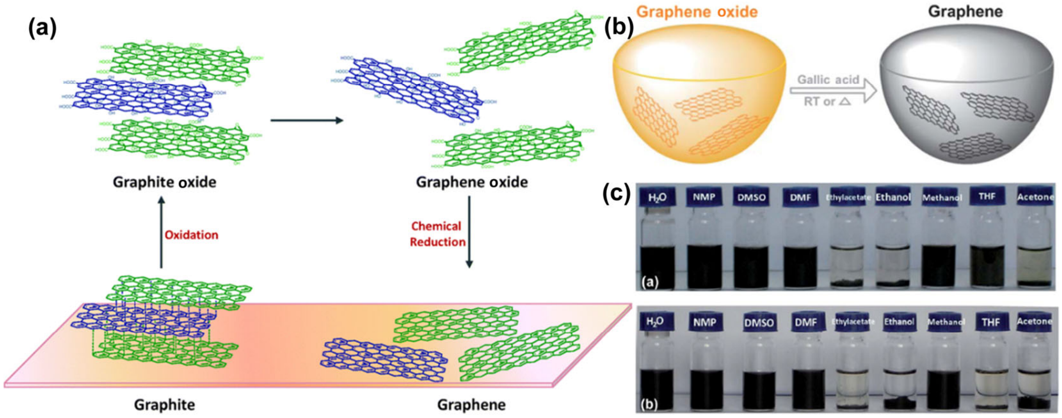

Figure 3 (a) The path of graphene preparation by chemical reduction. Reproduced with permission from Ref. [45], © The Royal Society of Chemistry 2014. (b) The preparation process of GO to graphene. (c) The GO are dispersed in different solvents. Reproduced with permission from Ref. [54], © The Royal Society of Chemistry 2013.

prospect in the industrial production of graphene, as well as emphasizing environmental friendliness, the research on reductant of GO chemical reduction method still requires a further development. It can be confirmed that although the chemical reduction method exists some defects, it is still to be considered as a comprehensive method of graphene production with the specific reduction mechanism.

2.1.3 *Chemical vapor synthesis*

Somani et al. firstly synthesized multilayer planar graphene by simple thermal CVD. Different from the methods we summarized above, the CVD belongs to the "bottom-up" synthesis mechanism, which is in the opposite solution with the structural defects of vital importance [69, 70]. Here we overview the process and reaction mechanism of the graphene synthesis by CVD in detail.

Generally, transition metals are used as substrates due to reducing reaction energy barriers [71]. A variety of transition metal substrates have been studied, including Ni [72], Cu [73], Ru [74], Ir [75], Pt [76], Co [77], Pd [78] and Re [79]. Different solubility and growth conditions of carbon in these transition metals can accurately affect the thickness and surface characteristics of graphene.

Since different transition metals weakly effect, the results in the conditional growth for the substrate reaction, copper can be used as the reaction substrate to describe the steps of synthesizing graphene by CVD synthesis. In 2009, Li et al. produced high quality and well-proportioned graphene films on copper foil with the progress of annealing in a hydrogen environment at 1,000 °C [73]. It is noteworthy that the solubility of carbon in copper was very poor, as a result, graphene could be used as a reaction substrate with large size and uniform thickness. Meanwhile, the graphene monolayer covered by the copper surface could reach more than 95%. Visibility, copper was more promising for preparing graphene by CVD comparing with other metals.

There are lots of researches on selecting suitable carbon sources by CVD method, including methane, methanol, ethylene and ethanol [80]. Here we summarized the detail synthesis process and mechanism of CVD. In fact, among the carbon sources, methane is a highly stable saturated molecule, which is usually used to provide initial accumulation of carbon initially. The route of synthesizing graphene by CVD requires methane to be adsorbed on the surface of the substrate, and then methane is dehydrogenated so that carbon can diffuse on the metal surface to generate graphene [81]. In recent years, the research is no longer simply confined to the supply gas of carbon source. By introducing liquid and solid carbon sources, the temperature and energy required for reaction decomposition can be studied [82]. In 2010, Srivastava et al. reported that the uniform and continuous graphene film with large surface area was synthesized on polycrystalline copper foil using liquid precursor hexane [83]. Zhang et al. discovered a two-step CVD method in which toluene was used as a carbon precursor to produce a continuous monolayer of graphene on the copper foil surface [84].

Previous scholars have also synthesized graphene catalyzed by metal. For example, by controlling variables to change the performance of graphene synthesis, Huet et al. fabricated high junction graphene on polycrystalline and epitaxial copper film respectively, finally found that graphene grown on epitaxial copper could reduce the structural defects with excellent performance on catalytic synthesis of graphene monolayer [85–87]. The experiment on Cu-Ni alloy also showed a very promising dissociation rate of carbon containing precursor.

In addition to research the influence of fixed parameters on graphene preparation with metal purity substrates, the effect of dynamic parameters in experiment including pressure, temperature, ratio of precursor gas, flow rate and residence time [76]. In 2011, Liu et al. reported the excellent properties of high purity copper in graphene monolayer synthesis [88]. After that, the influence of dynamic parameters on the experimental results is still worth discussing. The effect of the experimental parameters is not only reflected on an independent basis, but also interacted with each other to base on the parameters. Such as the effect of CH_4/H_2 ratio, annealing time and cooling rate on the preparation of graphene.

The adjustment of parameters in the CVD synthesis path will result in structural and performance gaps in the final synthesized graphene. CVD can adjust synthesis conditions in terms of controlling the number of layers and area. In order to obtain practical applications in various environments, one of the critical factors is that the synthesis can be completed at low temperature, so as to avoid structural defects (cracks, wrinkles) during the transfer process and the pollution of corrosive liquid on graphene [89].

In 2015, Yan et al. fabricated graphene sheets with GO via popcorn transformation at 180–220 °C. The experimental results still have excellent repeatability even under the conditions of air or inert gas. At the same time, the prepared graphene sheets with $400\ m^2\cdot g^{-1}$ showed an enhancement of about 300 times comparing with the pore volume of GO. It was found that blowout phenomenon was highly related to the oxygen content in GO. Moreover, they further proposed a three-step method for preparing metal nanoparticles to be loaded on graphene synthesized by explosion method, which was impregnates metal salt onto graphene (Fig. 4). Four different metals (Pd, Pt, Ni and Mn) were selected to prove the effectiveness and universality in practical application. At the same time, the prepared composite material had good dispersibility

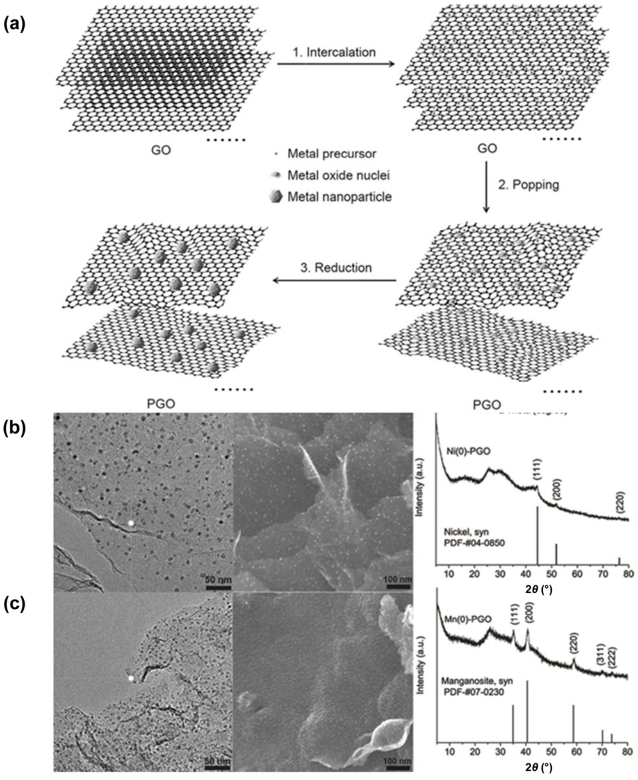

Figure 4 (a) Synthesis route of metal nanoparticle catalyst supported by popping of graphite oxide (PGO). (b) TEM image, SEM image and XRD pattern of Ni(0)-PGO. (c) TEM image, SEM image and XRD pattern of Mn(0)-PGO. Reproduced with permission from Ref. [90], © WILEY-VCH Verlag GmbH & Co. KGaA, Weinheim 2015.

and high load of nano metal ions. Under the concept of green chemical method, graphene had a very promising application potential [90].

2.2 Graphene from renewable carbon sources

Graphene is currently one of the most valuable and attractive materials with the properties of efficient, low-cost and green synthesis. Hydrocarbons are usually used as carbon sources for graphene synthesis. However, the ingredient is expensive, toxicity and flammability, which is not suitable for industrial production. Therefore, the basic requirements for seeking carbon sources must be convenience, low cost and environment protecting. Kalita et al. synthesized large-area graphene sheets by camphor plant derivative [91]. Zhang et al. fabricated high-quality graphene by ferric chloride and glucose [92]. Interestingly, Nguyen et al. proposed that graphene could be prepared by CVD with six carbon-containing materials on the back of copper foil, namely biscuits, chocolate, grass, plastic, cockroaches and dog dung [93]. These methods provide further development for promoting the commercialization of graphene.

2.2.1 Graphene synthesis from biomass (Shewanella, Escherichia coli, Sugar)

Recently, the research on graphene synthesis has mainly focused on the attempt to reduce the reducing reagent of GO in order to satisfy the principle of green economy. Biomass is used as a substitute for traditional reducing agents, such as *Shewanella*, *Escherichia coli*, sugar and other environmentally friendly reducing agents. *Shewanella* is a heterotrophic and anaerobic microorganism, which can live in all kinds of fish and sapropels. We can use arsenate and metal oxides (such as chromium, uranium, iron, and manganese) as terminal electron receptors in metabolic pathways. Moreover, heavy metals produced in the reaction process can be well precipitated in insoluble by this microorganism [94, 95]. Salas et al. first studied the reduction of GO by Schwarzschild cells in an anaerobic environment in 2010 [96]. In addition, Zhang et al. also used *Bacillus* to synthesis GO nickel sulfide network, which provided a broad-prospect in the application of supercapacitor materials (Fig. 5(a)) [97]. Guruantan et al. reported the reduction of GO by *Escherichia coli* in an aqueous medium at 37 °C [98]. Figure 5(b) showed the biomass of yellow-brown GO dispersion, RGO with Escherichia coli, and bacteria inhibitor added *Escherichia coli*, respectively. It is found that the GO reduced by *Escherichia coli* had satisfactory dispersion state (Fig. 5(c)), the size was twice than that of pure GO (Fig. 5(d)). Combining the two significant features of Raman from Fig. 5(e), the RGO with *Escherichia coli* had higher G/O intensity. The relative change in intensity showed that the number of sp^2 domains increased after *Escherichia coli* treatment. Graphene synthesis with glucose is a bottom-up method, and there are no harmful substances in the whole synthesis route. Meanwhile, the oxidation products can be used as the end-capping agent. Dong et al. found that glucose could promote the graphene synthesis in the alkaline environment. Glucose was firstly oxidized to aldose acid, further converted into ester, and final generate to oxygen-containing radicals, including hydroxyl and carboxyl groups. These oxygen-containing radicals could form hydrogen bonds with the oxygen-containing radicals on RGO [99]. In order to find environmentally friendly, efficient and low-cost reducing agents, there are still many directions to be explored, either in the selection of reducing agents or choice of synthesis path.

2.2.2 Graphene synthesis from other alternative resources (vitamin C) bio-precursor reduction method

Hydrazine derivatives are the common reductants in the preparation of chemically RGO. However, the promotion of these reductants is greatly limited by the toxicity of reaction products. Although they are satisfied the requirements of green and pollution-free, there is still some limitation to the product high yield of graphene. Therefore, the additives need

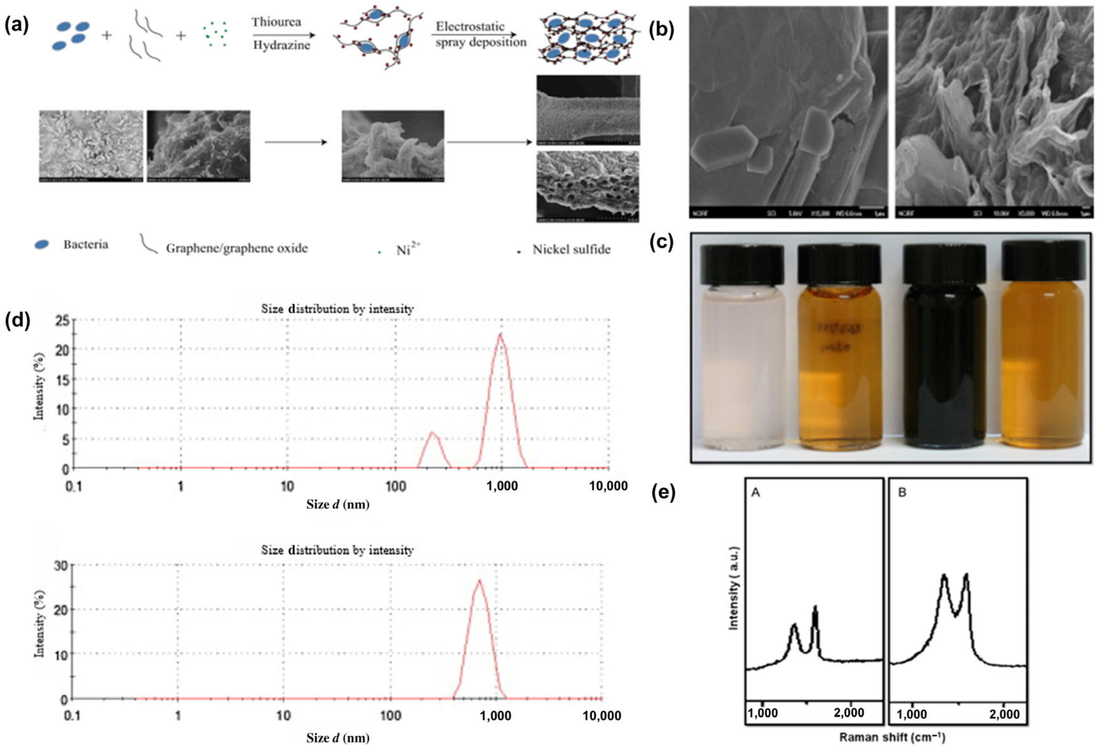

Figure 5 (a) Green synthesize of bacteria-reduced GO-nickel sulfide networks. Reproduced with permission from Ref. [97], © American Chemical Society 2013. (b) Dispersion photos of biomass, GO, *Escherichia coli* reduced GO (ERGO) and inhibitor pretreatment GO. (c) Digital photograph of GO and ERGO. (d) Size distribution of GO and ERGO. (e) Raman spectrum of GO and ERGO. Reproduced with permission from Ref. [98], © Elsevier B.V. 2013.

to be added to bring additional functional groups or capping agents to adhere graphene. The synthesized graphene has the characterization of irreversible aggregation, material pollution and even electronic conductivity [100]. On the basis of environmentally friendly reducing agents, the research mainly focuses on how to find a reducing agent compete with hydrazine. Among the current green reducers, L-ascorbic acid (vitamin C) has the advantage in the reduction capacity that can be used as end capping agents. Vitamin C plays an indispensable role in hydroxylation and reduction. It contains only three elements (carbon, hydrogen and oxygen) so that it can reduce the hazard of leading impurity atoms in the synthesis process. At the same time, as a green reductant, vitamin C promotes stable graphene suspension in the organic solvent. In 2010, a highly GO suspension was prepared by sodium borohydride, pyrogallol, vitamin C and hydrazine under alkaline conditions (Fig. 6(a)) [101]. Figure 6(b) showed the unreduced GO and vitamin C RGO stewing for 4 weeks in aqueous solution, respectively. After that, Gao et al. proposed a new preparation that vitamins as the reducing agents and amino acids as the stabilizers to synthesize graphene. The synthesis process is green, environment-friendly and non-toxic, which have a wide application prospect in the fields of bio-related sensors [102]. Nevertheless, because of that the ascorbic acid cannot completely reduce oxygen-containing radicals in GO, the preparation of graphene by biological precursors reducing agents still faces many challenges. In addition, the reaction mechanism and theoretical explanation are not clear enough that require continuous exploration.

2.3 Aqueous dispersible graphene

Dispersion stability is the decisive influence on the synthesis of graphene. The irreversible aggregation of graphene will generate in the absence of dispersant. Graphene layers tend to accumulate π–π to form a three-dimensional (3D) structure, and even convert into graphite. Therefore, in recent years, many researchers focus on how to disperse graphene in aqueous solution to provide more utilization of it.

It is reported that the stability of waterborne dispersed graphene is from the electrostatic repulsion. The influencing factors of the stability include pH value, electrolytic density and content of dispersed particles [103, 104]. Li et al. present a high-yield water-based graphene dispersion method that did not require high-yield water-based graphene dispersion method that did not require polymers and stabilizers. It was important to maintain stability of eliminating metal salts and acids from the system [105]. Konkena et al. also discussed the effects of varying pH and potential variables on dispersion stability. The RGO sheets formed a stable dispersing agent in a relatively alkaline medium with the pH value rang of 8–11.5 [106, 107].

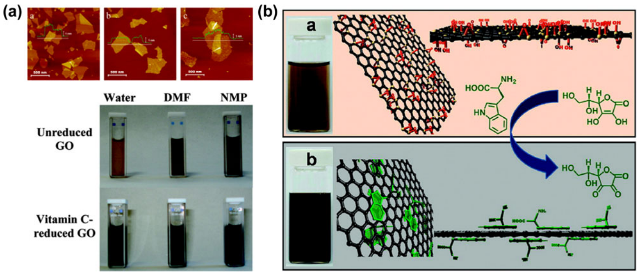

Figure 6 (a) AFM images of GO in different groups, and the photos of unreduced, Vitamin C RGO of water, DMF and NMP. Reproduced with permission from Ref. [101], © American Chemical Society 2010. (b) Schematic diagram of stable and dispersed graphene aqueous solution prepared by reduction. Reproduced with permission from Ref. [102], © American Chemical Society 2010.

Kashyap et al. tested the ideal range of pH value for stable dispersion of graphene using hydrochloric acid and sodium hydroxide solution. It presented an excellent stability when the pH value in the range of 7–11, which could be as the influencing factors of preparing graphene by water processing [108].

In the past ten years, some interesting attempts have been made in the aspect of adjuvants. Tian et al. prepared water-dispersible graphene with 2–5 atomic layers by one-step electrochemical method using graphite as the original material without additive [109]. Unalan et al. used polysaccharides to assist graphite exfoliation to form high-quality water-borne dispersed graphene [110]. In fact, how to maintain the dispersion stability of graphene aqueous solution is still a challenge. Liu et al. synthesized functionalizing water-dispersed high-quality graphene nanosheets with polydopamine, which can be used as electrode materials for miniature supercapacitors [111]. In addition, Bepete et al. has dispersed graphite to single-layer graphene that can be maintained for several months [112]. The stable dispersion has great potential to promote the application of graphene.

3 Applications of graphene in green chemistry

As the thinnest and hardest two-dimensional (2D) nanomaterial, graphene materials have the characteristics of ultra-light, superconductivity, excellent thermal conductivity, and good light transmission, which play an increasingly significant influence in traditional fields, such as aerospace, biomedicine and new energy. Based on these physical and chemical properties, it can be used as an important "additive" for industrial materials. Meanwhile, graphene has high electron mobility [113], extremely low resistivity, and fast electron migration at room temperature, which is expected to replace traditional semiconductor materials [114, 115]. In addition, the monolayer graphene present high transparency, and the absorption of visible light is only about 2.3% [116], which can replace the traditional material indium tin oxide in application fields such as displays and photovoltaics [117, 118]. Here, we mainly stand on the perspective of green chemistry to review the research of graphene application.

3.1 Energy storage applications

The current energy crisis and environmental problems caused by the continued consumption of non-renewable resources are further intensified. According to the development of industry, the combustion products of fossil fuels have caused irreversible global climate problem. Therefore, searching for new renewable resources and improving the utilization efficiency are the main problems that striving to solve. Due to excellent properties, graphene in energy storage applications has rapidly increased which can be used in energy storage, battery and supercapacitor.

Zhang et al. proposed a functionalized graphene nanosheet basing on polyethylene glycol and silver nanoparticles. The composite material could obviously improve the capability of absorbing visible light and photo-thermal conversion. The synergistic effect of polyethylene glycol and Ag nanoparticles could improve the thermal conductivity of the material to 95.3%, and the photo-thermal conversion rate could get to 88.7%–92.0%. In addition, the composite material had excellent performance in energy storage density, conversion rate, thermal stability and morphological stability, which had potential application prospects for the utilization of solar energy [119]. Khandelwal et al. reported a method by a simple hydrothermal method, in which alkylalkanolamine, triethanolamine and N,N-diethylethanolamine were used to simultaneous reduction without any surfactant. Compared with the original RGO, functionalized graphene had superior electrochemical performance, higher capacitance, excellent cycle stability and energy storage performance [120]. Ghaly et al. reported a material of V_2O_5 nanospheres and Fe_3O_4 graphene coated with 3D porous graphene for positive electrode and negative electrode respectively. The energy density was 45.9 $Wh·kg^{-1}$ and the power density could get to 898 $W·kg^{-1}$. At the same time, after 10,000 cycles, the capacitance retention rate was 89.6%, which had favorable energy storage prospect and further commercialization application [121]. Fang et al. reported a highly pleated graphene film prepared by Fe_3O_4 nanoparticles as template. The capacitance was as high as 370 $F·cm^{-3}$ in KOH electrolyte solution. In addition, 97% of initial capacitance could still be maintained after 10,000 cycles, providing the promising strategy for the industrial production of graphene [122]. The Fe_3O_4 nanoparticles graphene showed a highly folded morphology (Fig. 7(a)). At the same time, the observed fold formation ridges were inferred to be the reason for the stability of highly folded graphene. Figure 7(b) showed the CV curve from 5 to 100 $mV·s^{-1}$, which proved that the capacitance mainly from double-layer capacitance. From the galvanostatic charge/discharge curve (Fig. 7(c)), it showed a high degree of corrugation by adjusting current density, meaning that the graphene had excellent electrical properties as electrode materials. The performance of supercapacitors could be observed by controlling resistance and speed (Figs. 7(d)–7(g)).

Microcapsule phase change material is a tiny container containing phase change. In recent years, the requirements for the application of graphene functionalization energy storage are increasing. Chen et al. used melamine formaldehyde and octadecylamine to synthesize octadecylamine grafted GO by *in-situ* polymerization. The thermal conductivity was obviously improved on the basis of excellent dispersibility. When the microencapsulated phase contains 5% modified graphene, the thermal conductivity could increase to 38.52%, which would have great potential in the territory of thermopower deposit and temperature regulation [123]. Samantara et al. reported a one-dimensional mesoporous rod-like $NiCo_2O_4$ structure grown on RGO layer. It could be widely used as electrode materials in the supercapacitors, with small Tafel slope, good reaction kinetics and excellent energy density [124]. Liu et al. reported a method of preparing self-supporting flexible electrodes with high-quality graphene nanowires grown on graphene film. The assembled graphene nanowires could be used as electrode of the lithium-ion batteries. The reversible capacity could be 301 $mAh·g^{-1}$ at 1 C rate, while after 1,000 cycles there was still no attenuation. It opened a new way of graphene as anode in energy storage devices-batteries [125]. Deshmukh et al. reported a kind of matrix filled with polyvinyl alcohol, vanadium pentoxide and GO [126]. A novel ultra-high composite material was successfully prepared by colloid processing technology. The composite material had extra high specific inductive capacitance and low dielectric loss, which could be considered as an embedded capacitor to be applied in industry. It also provided a brand-new idea for developing ultra-high dielectric constant composite materials. Bashir et al. had made an interesting graphene combination with energy storage applications and construction [127]. By controlling the mass fraction of the nanocomposites, the beeswax/graphene nanocomposites increased to 22.5% with the latent heat of 0.3 wt.%. The thermal conductivity coefficient was 2.8 $W·m^{-1}·K^{-1}$, which indicated that the composite materials showed a great potential in reducing building energy consumption. Considering the current tense situation of the global energy, the application of graphene energy storage materials is one of the most popular research topics in the world. However, although there are numerous researches on the storage applications, graphene, as an important participant, still needs to further explore the specific reaction mechanism. Meanwhile, it is still not mature enough from synthesis to the application in industry.

3.2 Green catalysis

With the specific surface area, excellent modification and adsorption, graphene is playing an increasingly important role as a catalyst and carrier in the field of green chemistry. It has exhibited high catalytic activity without by-products, as well as the advantages of high cycle, extraordinary selectivity and stability. In 2016, Vineesh et al. found that Ni doped graphene sponge had low overpotential, small Tafel slope and faraday

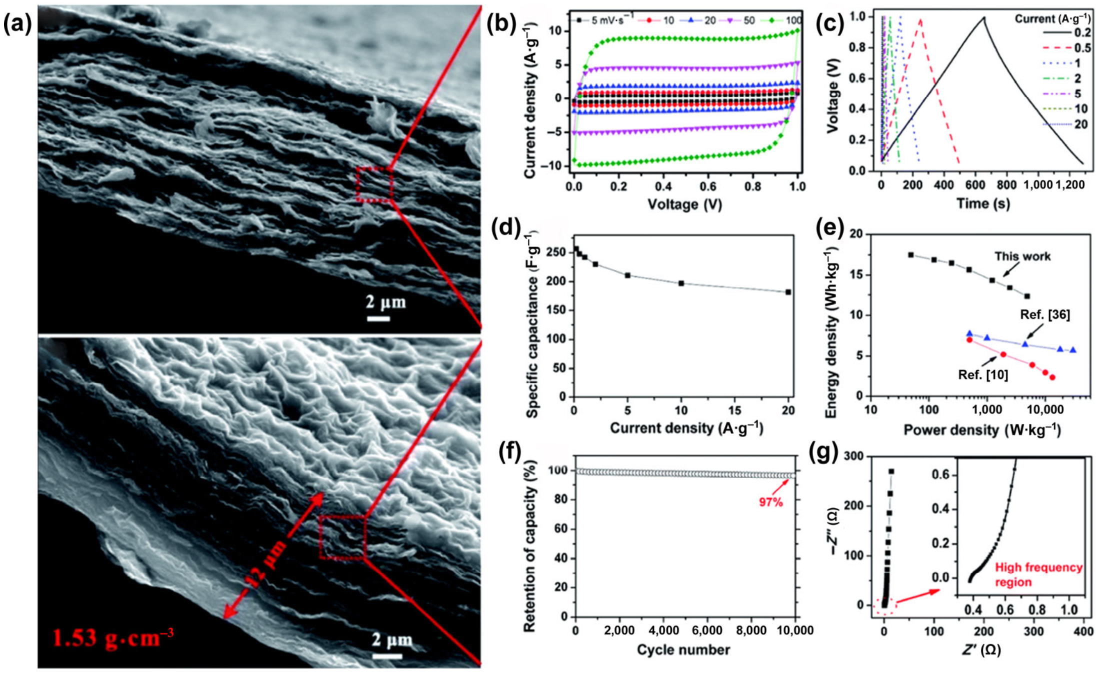

Figure 7 (a) SEM images of Fe_3O_4-RGO with highly wrinkled graphene film (HGWF). (b) Electrochemical capacitive performances. (c) Galvanostatic charge/discharge of different current densities. (d) Current density of HWGF. (e) Ragone plot of the two-electrode supercapacitor. (f) Cycling stability of HWGF. (g) Nyquist plots of HWGF electrode. Reproduced with permission from Ref. [122], © The Royal Society of Chemistry 2019.

efficiency [128], which had great prospects for sewage treatment and air purification. Zhang et al. proposed a new adsorbent grafted graphene synthesize method by ion exchange in aqueous solution, which provided an effective adsorption design approach [129]. Sahraei et al. synthesized the new magnetic biosorption hydrogel beads by gel method. It had a broad prospect in the field of water purification [130]. Li et al. prepared GO/polyacrylonitrile composite nanofiber membrane by electrospinning method [131]. The olive-like structure could greatly reduce the PM2.5 with the removal rate of 99.97%, which could play an indispensable role in air filtration performance.

3.2.1 *Thermal catalysis*

Graphene, with the characteristics of high specific surface area, excellent electron mobility and thermal stability, is considered to be an ideal catalyst [132], which has a broad application prospect in the field of thermal catalysis.

In recent years, graphene-based catalysts had made considerable breakthroughs in the application of thermal catalysis. Lin et al. reported a high-quality Pt/RGO as an *in-situ* catalyst. The products could significantly improve the pyrolysis of xylan, which had a good effect on the deoxygenation performance of furan products [133]. In 2015, Lan et al. proposed a sol-gel method to synthesize graphene/Fe_2O_3 aerogels, and studied the catalytic thermal decomposition performance of ammonium perchlorate [134]. Wang et al. reported a one-step hydrothermal method to modify RGO/$ZnFe_2O_4$ as catalyst, which could promote the heterogeneous reaction rate when the thermal decomposition temperature reduced [135]. In addition, Zu et al. prepared a GO-$MgWO_4$ nanocomposite and studied the catalytic effect on the thermal decomposition of cyclic trimethylene trinitramin (RDX) by controlling the ratio of GO to $MgWO_4$. Obviously, GO-$MgWO_4$ nanocomposite had an ideal performance as a catalyst [136]. Liu et al. successfully prepared GO-based nano-metal composite oxide $CuFe_2O_4$/GO, and studied the catalytic activity of $CuFe_2O_4$/GO nanocomposites for RDX thermal decomposition [137]. Meanwhile, Chen et al. reported an intelligent catalytic system established by grafting GO onto gold nanoparticles with poly brush, so as to control the reaction rate [138]. Ali et al. synthesized chromium nanoparticles supported on RGO, and studied the catalytic activity for carbon monoxide oxidation at low temperature. The catalyst had high catalytic activity with efficiency and stability [139]. Moreover, Ma et al. reported that an atom-dispersed copper catalyst was supported on defective nano-diamond graphene, which showed excellent performance in conversion rate, selectivity and stability [140]. Ma et al. also prepared a Pt nanocluster catalyst on the carrier of nano diamond/graphene composite core-shell material, which ensured the full utilization of metal atoms, high thermal stability and the best adsorption/desorption behavior. In the direct dehydrogenation reaction of n-butane, the selectivity of olefins finally reached 98% [141]. Karimi et al. have sensitized a Ni/Mo graphene catalyst in hydrocracking catalyzer. Compared with the industrial catalyst, the heterogeneous catalyst could improve the conversion rate of n-hexadecane hydrodesulfurization to 48%, which could reduce the deposition of carbon to inhibit the catalytic activity [142].

3.2.2 *Electrocatalysis*

Graphene has been widely used in the field of electrocatalytic energy conversion, including hydrogen evolution, oxygen reduction, nitrogen reduction and carbon dioxide reduction reaction [143, 144]. In fact, due to the stability and low density of electronic states near Fermi level, pure graphene is chemically inert, which is not ideal for catalytic applications. Therefore, it is necessary to introduce defects and heteroatoms to change chemically inert by doping heteroatoms can produce the effect of spacing graphene between layers [145]. In 2011, Zhang et al. synthesized monatomic platinum catalyst with excellent catalytic performance in the reaction of CO for the first time, and proposed single atom catalysis (SACs) [146]. Graphene as a substrate can provide high surface area and abundant anchoring sites for SACs, effectively preventing the agglomeration of SACs during the catalysis process [147]. Meanwhile, the outstanding electrical conductivity of graphene can also ideally complete electron transport. The applications in the field of electrocatalysis are of great significance.

In 2018, boron-doped graphene was synthesized by Yu et al. using thermal annealing of GO and boric acid [148]. After that, Wang et al. successfully prepared graphene-coated Co nanoparticles and embedded them into porous nitrogen-containing graphite carbon nanosheets, which had ideal durability and methanol resistance [149]. Yan et al. reported that graphene-manganese dioxide complex materials could be used as electrode materials for supercapacitors, which could undergo high-speed reversible redox reactions on the surface [150]. Gao et al. also prepared N doped activated carbons (GNACs) from graphene-polypyrrole composite material by alkali activation. The N, O functionalized surface with high capacitance and cycle performance [151]. Moreover, Jaffrey et al. proposed a thermal stripping method to prepare graphene nanosheets by nitrogen plasma body treatment [152]. The samples could be used as catalyst support materials for oxygen reduction reaction (ORR) platinum particles in proton exchange membrane fuel cells. So far, the doped graphene materials have shown excellent ORR performance. Currently, monoatomic catalysts have developed rapidly, the research is concentrated on the activity, selectivity and stability. How to effectively play a role under specific reaction conditions still needs to be discussed. Based on the SACs, Yan et al. discussed the application of SACs both in the energy conversion stability and catalytic activity. Whether to propose single atom electronic structure and coordination environment, or the detection method for comparison of catalysis, it was important for graphene to support metal atoms as a catalytic base in the field of catalysis (Fig. 8(a)) [153]. Li et al. demonstrated unique Ni-N_4 site through topological chemical conversion strategy, which illustrated high activity and selectivity in the process of carbon dioxide emission reduction [154]. The nickel-loaded metal exhibited the lower reaction energy barrier with favorable catalytic activity, meanwhile, the Ni-N_4-carbon appeared high selectivity to CO_2 (Figs. 8(b) and 8(c)). However, the stability of single-atom catalysis is also an important role in the application. The methods were proposed to improve the catalysis based on this strategy, including electric field, electric potential and mechanics. Single atoms could not exist stably and tend to form nanoparticles with better stability. Therefore, the ionic liquid treatment methods were raised to form a better stability between the metal and carrier [155, 156].

3.2.3 *Photocatalysis*

Recently, by using graphene-based nanocomposites as photocatalysts to utilize solar energy is regarded as one of the effective ways to overcome the energy consumption problem. For the first time, Fujishima et al. discovered that electrochemical photolysis of water could occur more effectively compared with platinum electrodes on titanium dioxide (TiO_2) electrodes [157]. Since then, the research on photocatalysis has grown rapidly. In 2008, Williams et al. successfully prepared well-separated TiO_2-graphene nanocomposites, which is a breakthrough for graphene-based nanocomposites as photocatalysts in the

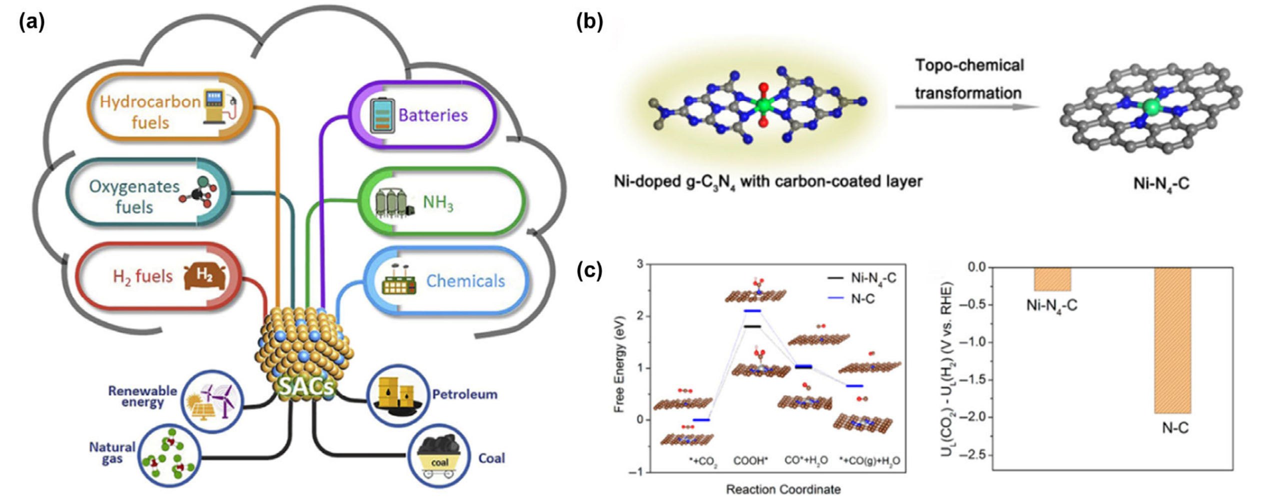

Figure 8 (a) Application field of SACs. Reproduced with permission from Ref. [153], © Elsevier B.V. 2019. (b) Schematic illustration of the topo-chemical transformation strategy. (c) Free energy diagrams of Ni-N_4-C and N-C. (d) Difference in limiting potentials of CO_2 and H_2 in reaction. Reproduced with permission from Ref. [154], © American Chemical Society 2017.

catalytic field [158]. After that. heterogeneous photocatalysis could be divided into three processes: absorption of incident photons, charge separation/transfer and surface charge utilization. The basic mechanism of heterogeneous photocatalysis and the research progress of graphene in photocatalytic field were reviewed in recent years [159]. However, some problems of photocatalysis are still controversial, including how to avoid the so-called photocatalysis caused by local heat generated. At present, the application of photocatalysis includes CO_2 reduction, H_2 generation and environmental remediation. As a result, the comprehensive understanding of photocatalytic mechanism and improvement of photocatalytic activity need to be contributed to the practical application of graphene-based nanocomposites.

Bie et al. reported a nitrogen-doped graphene grown on cadmium sulfide hollow spheres. It has realized seamless contact between photocatalyst and cocatalyst, which could promote the large-area transmission interface to improve the photocatalytic transmission interface to improve the photocatalytic activity [160]. Xu et al. also studied the process of improving electron separation/transfer by photocatalytic reduction of CO_2 with $CsPbBr_3$/GO. The electron consumption rate was increased to realize CO_2 reduction with high stability and efficiency [161]. In 2019, Wang et al. synthesized porous graphene/ZnO nanocomposites to study photocatalytic degradation. The nanocomposites could degrade methyl orange 100% in 150 min under natural light irradiation [162]. Meanwhile, Zhu et al. reported the photocatalytic reduction of CO_2 by graphene under sunlight and ultraviolet light respectively, which found a unique way to improve the photocatalytic activity of GO [163]. Jiang et al. also prepared nitrogen-doped TiO_2/graphene aerogel composites by chemical reduction self-assembly method. The products had excellent adsorption performance and visible light photocatalytic ability [164]. Dong et al. successfully synthesized graphene/Bi_2WO_6 nanocomposites with macroscopic three-dimensional structure by *in-situ* hydrothermal method [165]. Moreover, Jiao et al. proposed a surface one-step method to prepare a TiO_2/graphene composite catalyst [166]. We also prepared ZnO nanotubes on transparent flexible graphene substrates via hydrothermal preparation method [167]. The composite with high photocatalytic performance would have great application prospect in photocatalytic devices.

In recent years, graphene composites have been widely used in the fields of thermal catalysis, electrocatalysis and photocatalysis. Theoretically, as a catalyst carrier, graphene has a very ideal performance comparing with traditional catalysts. With the rapid development of computational chemistry, the design of catalysts has been further advanced. Nevertheless, the promotion of graphene catalysts to industrial applications still faces many challenges. Both the performance and the synthesis process are important issues that need to be resolved in future.

3.3 Electrochemistry

Graphene has particular physical and electrochemical properties, including ballistic conductivity, flexibility, high-intensity, large superficial area and rapid non-uniform electron transfer, which makes it having comprehensive prospects in electrochemical applications. Electrochemistry develops vital function in sensors, batteries, biological detection and electrocatalysis. Graphene has very high participation, especially electrochemical reaction mechanism, including electrochemical potential window, electron transfer rate and redox potential [168, 169]. Here, we summarize graphene as important participants in the field of electrochemistry, and provide inspiration for the future development direction.

The remarkable surface area ratio and electronic characteristics of graphene make it easy to detect the surface intermolecular changes, which is crucial for the application of sensors. More importantly, the large number of edge planes/defects are the main factors for electrodeposition kinetics, active electrocatalysis and biosensing performance [170]. Lou et al. reported a 3D film platform self-assembled from natural viscoelastic and conductive material RGO, which had excellent performance with high sensitivity and low detection limit [171]. In addition, it remained stable for a long time under 100,000 cycles and in a short reaction time of 5 milliseconds, which could be applied to the manufacture of varistor pressure sensors. Huang et al. reported that single layer GO was prepared by ink jet printing on the flexible substrate of polyethylene terephthalate, polyimide and paper [172]. The graphene pattern showed high electroconductibility after thermal reduction treatment, and the conductivity did not decrease after 100 repeated bending cycles. It also showed very sensitive to hydrogen peroxide (H_2O_2) and excellent circuit properties. Mansouri et al. proposed a novel glucose sensing nano-biological composite membrane. The glucose oxidase immobilized on the 3D graphene membrane was used as a glucose bioanalytical sensing platform. The biosensor presents outstanding sensitivity and response performance. In addition, it had excellent repeatability and long-term stability, which could be used to detect human serum samples

[173]. Shang et al. prepared multilayer graphene nanosheet electrode by catalyst-free microwave plasma [174]. This electrode had favorable performance in the resolution of amino acid, dopamine and uric acid, which has become an ideal choice to supersede traditional electrodes to solve the defects of dopamine selectivity and sensitivity. In addition, graphene-based materials with wide electrochemical window, high transparency, chemical resistance and excellent electron mobility can undoubtedly be considered as a good choice for electrode related electronic devices (batteries, supercapacitors, etc.). Based on the characteristics of high sensitivity, simple instrument, high operability and easy automation, graphene has a very promising application in the fields of biology, medicine, environment, food and industrial analysis. Goryacheva et al. reviewed microRNA detection using luminescent carbon nanostructures. The high π electron density of graphene could as a carrier for single-stranded oligonucleotides. Oxygen-containing functional groups (such as carboxyl) have a crucial effect on the dissolution of graphene. In addition, the size, defects, and the quantity of additives would all affect the luminescent performance. Based on the above influencing factors, carbon nanostructures used for microRNA detection are obviously excellent candidate materials. Meanwhile, the low cost and simple synthesis are more favorable for application and promotion [175]. Based on biocompatibility, flexible and electrical properties, Hébert et al. had studied spontaneous slow wave activity, sensory evoked response and synchronous activity in visual and auditory cortex of epileptic rat models [176]. Figure 9(a) showed that 20 neural probes were added to the graphene solution gated field effect transistor. On the basis of ensuring the adhesion of the cell, a release-type free-standing neural probe was manufactured. The ratio of graphene field effect transistors was higher than that of PEDOT: PSS poly(3,4-ethylenedioxythiophene), which had obvious advantages of low noise, flexibility, stretch ability, biocompatibility and excellent nerve recording performance, providing a powerful tool for the cognition of internal nerve electrophysiology. Kanai et al. applied open-sandwich immunoassay for non-competitive detection of low molecular weight antigens graphene. The sensitivity had been increased by 100 times with a wider antigen detection range. It also had good sensitivity under the condition of human serum in the environment with a promising promotion prospect in medical diagnosis (Fig. 9(b)) [177].

Although there are many researches on the electrochemical properties of graphene, the reaction mechanism is still not comprehensive enough. The synthesis paths of graphene will affect the properties of samples, such as electronic properties, charge transfer mechanism and transfer density. At present, the electrochemistry application conditions of graphene-based 2D materials in industry are still immature, further explorations are needed in terms of reducing costs, improving efficiency and practicability. However, according to the current research progress, the electrochemistry application performance of graphene is still worthy of expectation.

3.4 Fuel cells and supercapacitors

Fuel cells are energy storage applications that continuously translate chemical energy into electrical energy through electrochemical reactions between fuel (hydrogen, hydrocarbons, etc.) and oxidant. The fuel cell consists of negative electrode, positive electrode and separation membrane. It has the advantages of high-power generation efficiency, low environmental pollution and high specific energy. Moreover, there are some special characteristics for graphene as catalyst carrier: (i) significant specific surface leads to high dispersion degree of catalytic, (ii) chemical stability, electrochemical stability and high electroconductibility, (iii) the electrode can be easily recovered from the catalyst [178]. As a result, countless researches in fuel cell applications have been reported.

Platinum, gold and ruthenium are frequently used as cathode materials in fuel cells [179, 180]. Thus, the limited reserves of these metals will greatly confine the application of fuel cells. In 2003, Li et al. used multi-walled carbon nanotubes supported platinum as a catalytic agent in wood alcohol fuel cells, showing enhanced ORR activity and excellent cell performance [181]. In 2009, Gong et al. proposed perpendicularity arranged nitrogen-doped carbon nanotubes as non-metal electrodes, which showed better catalytic activity and stability in basicity fuel cells [182]. In order to avoiding expensive precious metals as catalysts finding an economic, efficient and pollution-free nonmetallic catalyst has been frequently researched. On the basis of high conductivity and surface area, graphene has been applied in the field of fuel cells.

Koo et al. first prepared RGO and then added to the cathode made of activated carbon, which could enhance the cathode performance and increase the power generation capacity of microbial fuel cells [183]. According to the different weight ratios of RGO, it could reduce the internal resistance of the cathode and enhance the electrical property. Luo et al. modified graphene-based materials to obtain nano complex

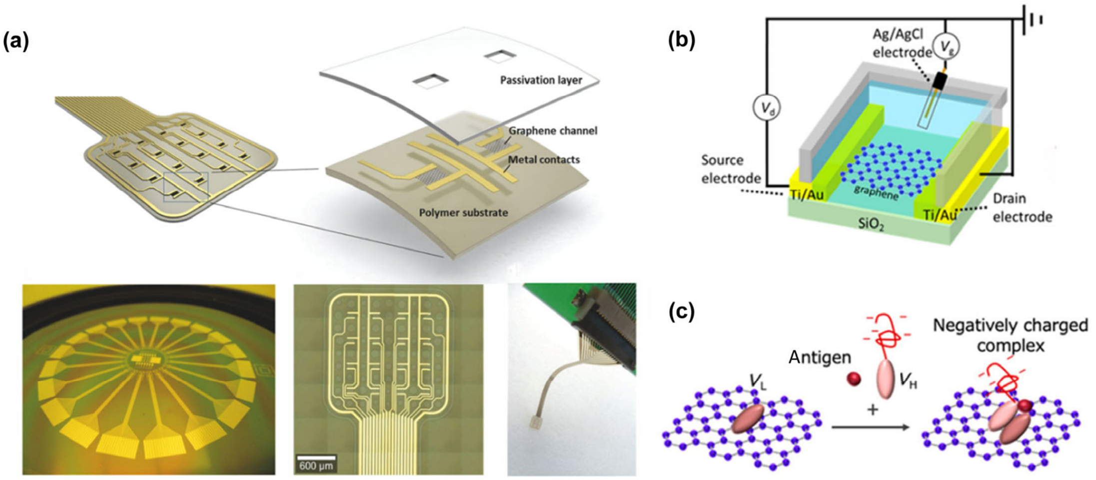

Figure 9 (a) Technology of graphene SGFET arrays. Reproduced with permission from Ref. [176], © Hydrogen Energy Publications LLC. Published by Elsevier Ltd. 2016. (b) Field effect transistor and open-sandwich immunoassay. Reproduced with permission from Ref. [177], © American Chemical Society 2020.

material for anion interchange battery [184]. Compared with common quaternate polysulfone membranes, the composite membranes had high water absorption, strong tensile strength, large elongation and good stability in alkaline solution. Papiya et al. synthesized NiCo/GO nanocomposites by silane modification of GO [185]. As potential cathode catalysts for microbial fuel cells, the power density was 2.1 times higher than platinum/carbon, showing great application prospects for ORR industrial cathode catalysts. Pothaya et al. had prepared Pt/C catalysts for polymer electrolyte membrane fuel cells using strong static electricity adsorption technology, which present high anti-agglomeration/sintering properties [186]. It would be potential value for prolonging the service time of proton exchange membrane fuel cells. Qu et al. reported a simple CVD method to prepare nitrogen-doped graphene as a nonmetallic electrode, which greatly improved the reaction efficiency of oxygen reduction in fuel batteries [187]. Compared with Pt/C electrode, it exhibited better electrocatalytic activity, as well as long-term stability, cross-resistance and toxicity of oxygen reduction. More importantly, it could be obtained inexpensively with large scale. Traditional fuel cell design requires strict guarantee of the interface between the two-pole electrolytes. Yang et al. proposed a flexible miniature fuel cell operating with 3D nickel foam and RGO as the positive and negative electrode, respectively [188]. The flexible fuel cell had high power density with good stability and consistency. Yang et al. reported a kind of palladium nano-plate using graphene as catalyst for methanol fuel, which had good electrocatalytic activity, stability and tolerance [189]. Yousef et al. prepared multilayer graphene/nickel nanocomposites as the active anode of fuel cell [190]. Yi et al. proposed a one-pot pyrolysis method of compound iron monoatomic (FeSA-G) on graphene [191]. The strong interaction between platinum and phosphate had adverse effects on the agglomeration of platinum/carbon catalysts at high temperatures. Compared with platinum carbon cathode, the high stability and tolerance of ferrous sulfate cathode catalyst were important factors for the stable output power of fuel cells. Ferrous sulfide catalysts could replace platinum carbon catalysts at high operating temperatures. Figure 10(a) showed the size of the Pt/C catalyst grains increased from 3.4 to 6.3 nm after 100 h of polarization. At the same time, Fe single atoms were evenly distributed and well dispersed on nitrogen-doped graphene at high temperatures. Figure 10(b) showed the electrochemical activity of Fe supported nitrogen-doped graphene, which present low cycle density, high catalytic performance and excellent resistance. When the temperature rises to 230 °C, FeSA-G as a catalyst, exhibited excellent operating performance (Fig. 10(c)). Meanwhile, the stability would be increased by controlling the voltage and battery density.

Hou et al. used a binder to combine graphene and carbon fiber as a cathode for the first time, which was applied to the battery to increase the specific area of the cathode and improved the electrochemistry performance. The fuel cell had excellent performance in the simulated marine environment, which could be very resistant to seawater immersion for a long time with mechanical stability. It showed great potential application value in marine power supply equipment components such as submarine sensors [192].

Graphene derivatives are widely used in fuel batteries as promising substitutes, playing a vital role in anion exchange membranes, electrodes and catalysts. With the participation of graphene, the concept of fuel cells has been further expanded in innovation. It can be predicted that graphene, as an important participant in the field of fuel cells, still has considerable development space, including catalytic performance, application of environment and further reduction of production costs.

Supercapacitors, as energy storage components, have the advanced of fast charging, discharging characteristics and energy storage. Compared with traditional capacitors and batteries, supercapacitors are widely used in electric vehicles and portable supercapacitors, as energy storage components, have the advanced of fast charging, discharging characteristics and energy storage. Compared with traditional capacitors and batteries, super-

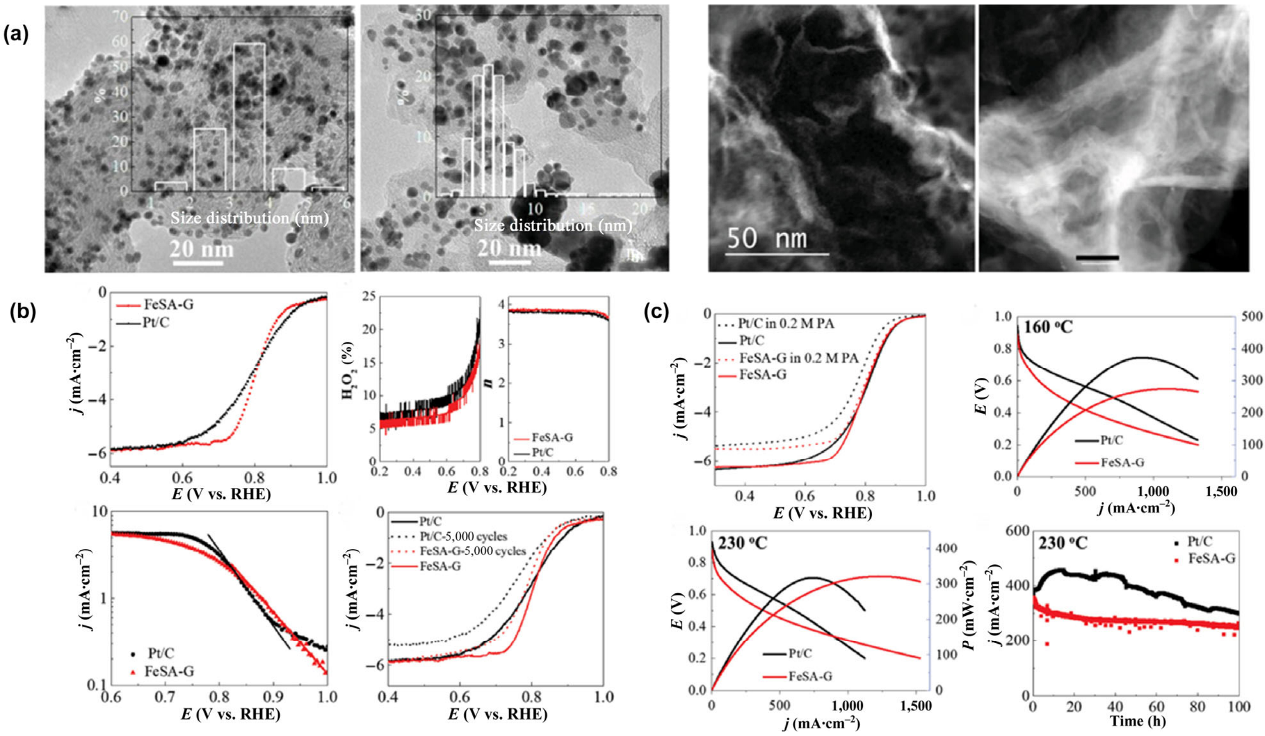

Figure 10 (a) TEM image for the cell with Pt/C and FeSA-G cathodes. (b) Detection of oxygen reduction reaction performance. Including linear scans voltammetry (LSV) of FeSA-G and Pt/C, H_2O_2 yield and electron transfer number during the ORR process. (c) Detection of phosphate resistance and fuel cell stability performance. Reproduced with permission from Ref. [191], © Cheng Y., et al. 2019.

capacitors are widely used in electric vehicles and portable electronic products. As a result, graphene with high specific area, excellent ecroconoucubuty and mechanical character that can be the preferred material for supercapacitors. The research of graphene supercapacitor mainly focuses on energy and power.

Energy storage capacity is the concentrated expression, which directly determines the working time of supercapacitor. In theory, by enlarging the specific surface area of electrode is the main effective way to increase capacitance. The speed of energy discharge and charging of supercapacitors depends on the power density, which are the main factors hindering the promotion of electric power [193]. According to energy storage mechanisms, supercapacitors are split into double-layer capacitors and pseudo-capacitors. The former accumulate charge through the electrode-electrolyte interface. Therefore, the key point is how to obtain high energy storage and reduction of resistance. However, the electrochemical performance and service life of pseudocapacitance are greatly limited by imperfect conductivity [194]. Recently, there are some research on the application of graphene participates in the supercapacitors, including the synthesis methods and electrochemical properties.

As an electrode material, graphene has excellent power density, yet its energy storage capacity is usually unsatisfactory. Ma et al. designed a mixture of 2D NiCo layered double hydroxides (LDHs) and zero-dimensional (0D) graphene quantum dots (GQDs) as electrode materials, which had high specific capacitance that could be used as toughening materials [195].

The GQDs/NiCo LDH had specific capacitance and cycle stability. It provided a breakthrough attempt to enhance the cyclic stability of pseudocapacitive electrode materials. Ramadan et al. proposed a hydrothermal method to prepare polyaniline/sulfur, nitrogen germanium quantum dot nanocomposites (PGQDx) by chemical *in-situ* polymerization process. By controlling the doping elements, PGQD20 exhibited a specific capacitance of 2,524 $F \cdot g^{-1}$ with 100% excellent cycle stability after 1,000 charge cycles, which effectively reduced the resistance effect during charge transfer [196]. Lei et al. reported a sufficient improvement in the electrochemically active surface area of MnO_2 by reflowing graphite hollow carbon spheres in $KMnO_4$ aqueous solution [197]. It had ideal performance in electron transport, which could be used as electrode in asymmetric supercapacitors. In addition, after 1,000 charge/discharge cycles, the capacitance retention rate and Coulombic efficiency were 99% and 90%, respectively. Zhang and co-workers developed a conductive matrix from the pyrolysis of natural balsam wood [198]. The PWC/MnO_2/GQDs electrode was prepared by hydrothermal deposition with manganese dioxide and graphene quantum dots. At the same time, the retention rate of capacitance was 95.3% after 2,000 cycles, which provided a new attempt of energy storage materials and further promoted the development of energy storage applications.

One-dimensional graphene nanostructures are ideal in terms of conductivity, ion transport and stability [199]. Moitra and co-workers proposed a nano-composite material consisting of $BiFeO_3$ nanowires and RGO. As an electrode material, it had desired power density and charge density, which would be promising in the field of supercapacitors. Kou et al. reported a method for continuously spinning polyelectrolyte-coated graphene/carbon nanotube by coaxial wet spinning, which could be used as the safety electrode of supercapacitor. The high flexibility and braking made it have a promising application prospect in wear-resistant electronic products [200]. In addition, it has tremendous potential opportunities in the development of flexible supercapacitors. The increasingly microscopic and flexible portable electronic device revolution has further promoted the related research. The flexible asymmetric supercapacitor composed of manganese dioxide, titanium dioxide and activated graphene [201, 202]. Lei et al. prepared MnO_2-coated carbon nanotube (MnC) intercalated graphene composite material. The electrical performance of MnC/RGO was much higher than that of MnO_2/RGO. It could still be maintained at about 70% of capacitance retention rate after 1,300 charging cycles, and the Coulomb efficiency was maintained at 94%–96% [203].

In fact, 2D graphene structure has outstanding performance in conductivity, specific surface area and mechanical properties. Graphene is one of the candidate materials for flexible thin film supercapacitors in the future. Li et al. prepared flexible MnO_2/graphene film as the electrode of the supercapacitor, which has showed excellent electrochemical characteristics. Meanwhile, the capacitance did not decrease significantly after 10,000 cycles [204]. Tu and co-workers proposed a tungsten disulfide/RGO nanosheet using a molten salt process. As the electrode for supercapacitors, it has showed a specific capacitance as high as 2,508.07 $F \cdot g^{-1}$. After 5,000 cycles, the capacitance retention rate could still reach to 98.6% [205]. One main problem of 2D graphene is the aggregation between graphene layers, which ultimately hinders the performance of supercapacitor. In order to avoid this phenomenon, graphene-based metal oxide composites have been payed much attention. These metals include manganese [206], cobalt [207], nickel [208], ruthenium [209], titanium [210], zinc [211] and so on. Qiu et al. reported an ultrasonic treatment of GO compound using carbon as spacer. The capacitance of GO and carbon nanotube hybrid membrane was 140 $F \cdot g^{-1}$. It provided a more reasonable way for the long-term processability of for the application of carbon-based nanomaterials [212]. Yang et al. found that water spacer had quite an ideal effect in preventing graphene re-aggregation. It had great application value in limiting the formation of graphene re-stacking, as well as providing a reasonable development with higher energy density and power density [213]. What's more, there are also some researches on the unique electrode performance of graphene-metal oxide materials in supercapacitors. The composite materials can effectively reduce interlayer aggregation of graphene. Graphene materials with 3D structure have unique characteristics including porosity, superficial area, density, mechanical properties and electrochemical properties. In addition to further solving the problem of re-aggregation of graphene, it provided new possibilities for the application of bulk materials [214]. The 3D material has a multi-hole structure, which could increase the land area between electrode and electrolyte solution, providing an electron transfer channel on graphene [215]. 3D graphene skeleton mainly includes porous structural materials such as aerogel, hydrogel and, sponge [216]. Shah reported a sol-gel self-assembly technology to synthesize hydrogel electrodes. The shear modulus and mechanical integrity of the hydrogel were significantly improved. Meanwhile, it showed high specific capacitance and excellent multiplying power performance. The structural filler of the electrode was further enhanced, providing more possibilities for the development of multi-functional energy storage devices [217]. Zhou et al. synthesized layered molybdenum disulfide and 3D graphene composites by impregnation and drying method. The capacitance retention rate could reach to 110.57% under 4,000 cycles. This outstanding property speculation might be due to the increase of graphene interlayer spacing caused by layered molybdenum disulfide and discontinuous deposition, which would affect the transmission process of electrolyte cations. However, the specific reaction mechanism for improving electrochemical performance still needs further in-depth study [218]. Li et al. prepared porous carbon and Co_3O_4 composite materials by the pyrolyzing precursor of 3D graphene. The anoxic Co_3O_4 state enhanced the transmission of ions. This work provided a more practical application strategy for porous carbon/metal oxide hybrid type as electrode of supercapacitors [219]. Ramadoss et al. adopted a self-assembly strategy to prepare uniform 3D graphene powder on flexible graphite substrate by CVD, which exhibited excellent capacitance retention [220]. Meanwhile, He et al. synthesized a flexible 3D graphene network loaded with manganese dioxide as electrode. It provided an ideal method for the development of flexible supercapacitors [221]. The obvious porous structure was observed after the nickel template removed (Fig. 11(a)). The structural integrity was maintained at the same time. The CV curve indicated that the capacitance was mainly provided by double-layer capacitance at different scanning rates (Fig. 11(b)). Figure 11(c) showed the influence of mass contrast capacitance with different MnO_2 added. Due to the principle surface, there was low proton diffusion constant so that the degree of participation in pseudo-capacitance reaction was unsatisfactory. Meanwhile, the conductivity of MnO_2 also hindered the composite material. Figure 11(d) showed the relationship between specific capacitance and surface with different scanning rates. Obviously, MnO_2 could effectively promote energy storage capacity, which might be due to the highly porous structure.

Chen et al. proposed the application of hydrothermal synthesis of nitrogen-doped graphene hydrogel in supercapacitors. Organic amines were used to controllably adjust the internal and nitrogen content of graphene. In addition, the current density was adjusted to 100.0 $A \cdot g^{-1}$, and the capacitance retention rate was 95.2% under 4,000 charge/discharge cycles. It showed that organic amine could effectively improve the application of nitrogen-doped graphene in ultra-high power supercapacitor [222]. Graphene has shown an excellent application prospect as candidate material. This section summarizes the outstanding electrochemical characteristics and cycle stability of graphene structures as electrode materials, including structure control, preparation technology and electrochemical properties. However, it is still tough for graphene as a practical electrode material, as well as how to effectively overcome the stacking between graphene layers and the influence of defects on electrochemical performance. For example, the relationship between porous structure and electrode dynamics mechanism has been intensively studied, including macropores/mesopores, mesopores/micropores, macropores/micropores and macropores/mesopores/micropores. Macropores can serve as a buffer pool for the electrolyte to reduce the diffusion distance from the inner surface of the pores, while mesopores can provide available surface area for ion transport/charge storage [223]. Therefore, further research on the reaction mechanism of graphene electrode is one of the major issues to be solved at present, while finding a cost-effective working mechanism will play an important role in promoting the application of supercapacitors.

3.5 Biomedical application of biocompatible graphene

Due to the biocompatibility of graphene, the research in the biomedical field has been continuously expanded and deepened, including drug delivery, cancer treatment, biosensors and medical imaging. Firstly, graphene has high surface area to obtain drug loading. At the same time, graphene is modified with active oxygen-containing groups, thus it has the ability to promote the absorption and function of hydrophobic drugs. Meanwhile, it can also modify ligands with targeting function. These excellent properties of graphene promote it have great potential for biomedical applications.

Cancer therapy is currently one of the most concerning research topics in the global medical field. With favorable biocompatibility and stability, graphene can be predicted with application prospects and therapeutic effects on the biomedical field [224]. There are three methods for reducing GO as a drug carrier, including noncovalent interaction, covalent bonding, and hybridization with nanocarriers [225, 226]. In 2008, Liu et al. formed graphene as a drug carrier with aromatic drugs through simple adsorption, opening up a new idea for graphene in medical application [227]. Shang et al. used labelling metabolism and differentiation of neural stem cells to study its absorption and biocompatibility. After treated with graphene quantum dots, the proliferation, metabolism and differentiation of neural stem cells did not change significantly. It showed great potential on the principle of effectiveness and environmental protection [228]. Xie and co-workers proposed a new drug transport system composed of GO, protamine sulfate and sodium alginate. The prepared nanocomposite had high dispersibility, stability and inhibition adsorption of non-specific proteins in physiological environment, providing a

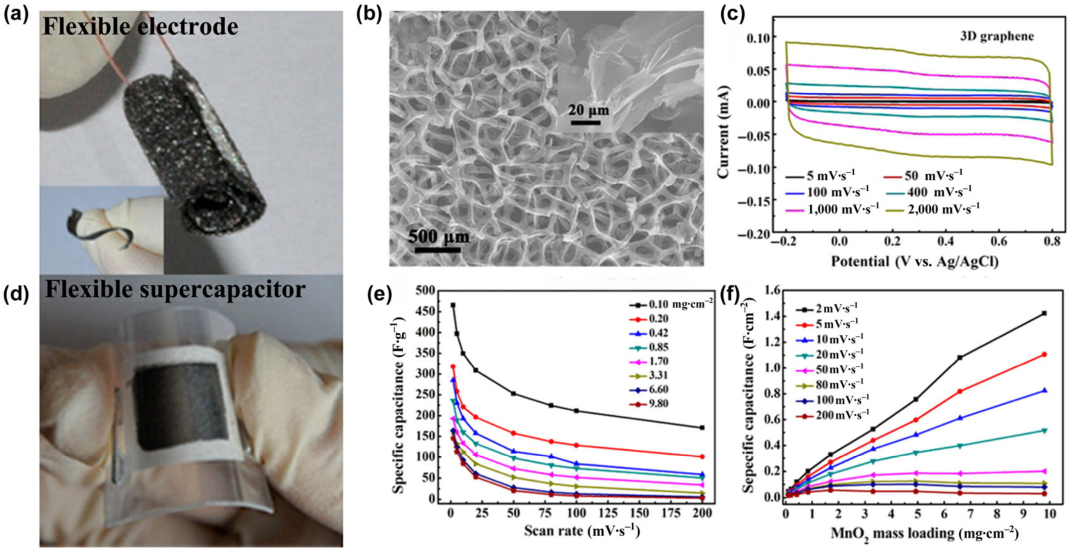

Figure 11 (a) and (d) Image of graphene-based flexible supercapacitors. (b) SEM image of 3D graphene networks after removal of Ni foam. (c) CVs of graphene network electrode. (e) Specific capacitance vs. scan rate for samples. (f) Curve of the relationship between areal capacitance and mass density of MnO_2. Reproduced with permission from Ref. [221], © Elsevier B.V. 2017.

broader application prospect of GO-based nanocomposite coated with natural polypeptide in biomedical field [229].

Gai and co-workers prepared reduced nano GO with low cytotoxicity based on establishing photothermal therapy (PT) as a platform. The nano-GO was proved to be feasible as a PT therapy. At the same time, under the action of the constant-wave near-infrared laser, the effect of reduced nano-GO on esophageal adenocarcinoma cells cultured *in vitro* was studied. It was confirmed that the nano-GO was guaranteed to treat tumors [230]. Geng et al. had prepared nitrogen-doped graphene quantum dots with a concentration of 50 $\mu g \cdot mL^{-1}$, which had high blood compatibility and low cytotoxicity. In addition, the composite material had nice imaging function for stem cells and significantly enhanced the differentiation of rat bone marrow mesenchymal stem cells [231]. Guo et al. blocked dendrimers with amino groups grafted onto GO nanosheets. GO was modified with gadolinium diethylenetriamine pentaacetate and prostate stem cell antigen monoclonal antibody. It had exhibited specific targeting to cancer cells and could deliver anticancer drugs to malignant prostate tumors [232]. Lima-Sousa et al. reported a new hyaluronic acid-based amphiphilic polymer to modify RGO, which had effectively improved the cell compatibility and the ability of target tumor therapy (Fig. 12(a)) [233]. Wang et al. used heparin as reductant to synthesize functional RGO in aqueous solution. The combination of heparin-RGO and drugs could achieve excellent carrier performance [234]. Dai et al. prepared multifunctional biocompatible nano-graphene oxides with various physical dimensions in a scalable manner. Anti-cancer drugs were loaded on NGO in large quantities and selectively transferred to specific cancer cells through antibody-guided targeting [235].

Muñoz and co-workers reported an electrochemical sensor based on nanocomposite materials with gold nanoparticles, biological recognition agent and RGO. Thyroxine was identified and detected by supramolecular chemistry. In order to judge the role of gold nanoparticles in identification and detection, the comparison of different ingredients was studied. It provided a reasonable strategy for the development of high efficiency and low-cost detection applications [236]. Yan et al. reported a one-pot synthesis method using CO reduction reaction to adjust the size of gold sulfide nanoclusters. Fine-tuning of gold nanoparticles at atomic level it was of important meaning for the expansion of application, including biosensors and clinical medicine [237]. The particle size of Au nanocluster's sulfide was correlated with pH value by ultraviolet-visible spectroscopy positively (Fig. 12(b)). Figure 12(c) indicated the production of Au-NCs by adjusting the pH value in the CO reduction method. Graphene-based materials applied to biomedicine still faces many problems for the real promotion in biomedical clinical applications due to the toxicity of graphene. The toxicity is decided by the factors of the size, shape, biological environment and concentration. In addition, there are many unclear problems in the inflammatory reactions that need further research. It has been found that graphene has adverse effects on the morphological development of organisms based on zebrafish embryos [238]. The interaction mechanism and absorption methods of graphene, as well as the circulation, accumulation and distribution can reduce the toxicity of graphene and provide constructive suggestion for biomedical applications.

4 Conclusions

The green synthesis of graphene has received excellent potential due to the advantages of high-efficiency, environmental-friendly and green reductants. RGO is currently more common green synthesis method including borohydride, biomass, plant extracts and even animals. Meanwhile, the unique applications of graphene provide a solid foundation for the development of environmental protection and renewable energy in the fields of energy storage, catalysis and biomedicine. As a potential material, graphene has the extensive application prospect in conductive ink, anti-corrosion coating, cooling materials, lithium batteries and ultracapacitors.

Although graphene has shown supernormal properties with great attention, there are still massive problems in the reaction mechanism and practical application, such as electron transfer, impurity dislodge, as well as defects and stability. Admittedly, based on the industry benefits, it still needs much attention in the practical application of graphene with higher efficient, more pro-environment and better functionality.

Acknowledgements

This work was financially supported by the National Natural Science Foundation of China (No. 51502166) and the Scientific Research Program Funded by Shaanxi Provincial Department (No. 17JK0130). Q. Y. acknowledges Chemical Engineering of National University of Singapore for the kind hospitality during her visit.

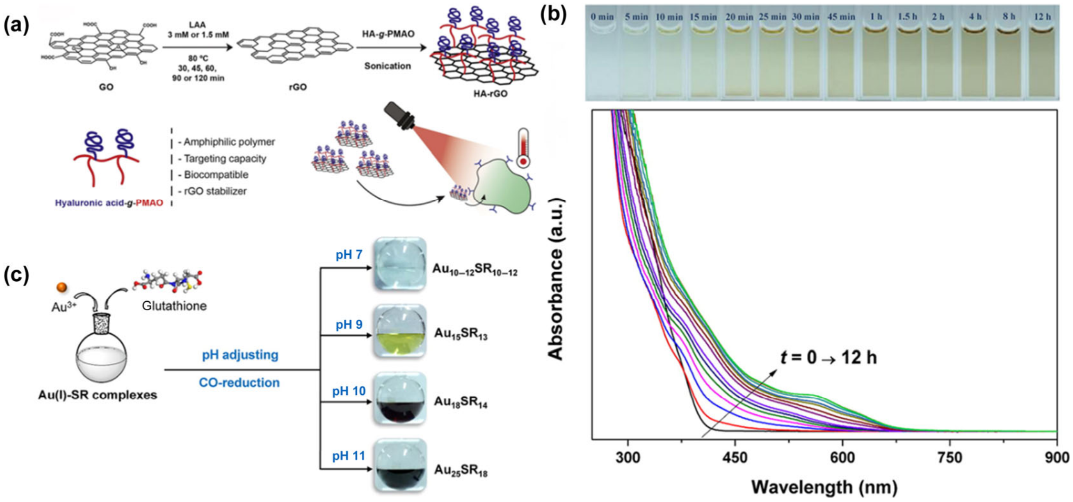

Figure 12 (a) Preparation of hyaluronic acid-reduced GO and the application in cancer photothermal therapy. Reproduced with permission from Ref. [233], © Elsevier B.V. 2018. (b) UV–vis spectrum of $Au_{18}(SG)_{14}$ NCs. (c) The synthesis of $Au_{(x = 10–12, 15, 18, \text{and } 25)}$ carbon nanofiber. Reproduced with permission from Ref. [237], © American Chemical Society 2013.

References

[1] Anastas, P. T.; Warner, J. C. *Green Chemistry: Theory and Practice*; Oxford University Press: Oxford, 1998.

[2] Novoselov, K. S.; Geim, A. K.; Morozov, S V.; Jiang, D.; Zhang, Y.; Dubonos, S V.; Grigorieva, I V.; Firsov, A. A. Electric field effect in atomically thin carbon films. *Science* **2004**, *306*, 666–669.

[3] Geim, A. K.; Novoselov, K. S. The rise of graphene. *Nat. Mater.* **2007**, *6*, 183–191.

[4] Smolsky, J. M.; Krasnoslobodtsev, A. V. Nanoscopic imaging of oxidized graphene monolayer using tip-enhanced Raman scattering. *Nano Res*. **2018**, *11*, 6346–6359.

[5] Geim, A. K. Graphene: Status and prospects. *Science* **2009**, *324*, 1530–1534.

[6] Allen, M. J.; Tung, V. C.; Kaner, R. B. Honeycomb carbon: A review of graphene. *Chem. Rev*. **2010**, *110*, 132–145.

[7] Ni, Z. H.; Wang, Y. Y.; Yu, T.; Shen, Z. X. Raman spectroscopy and imaging of grapheme. *Nano Res.* **2008**, *1*, 273–291.

[8] Kumar, R.; Sahoo, S.; Joanni, E.; Singh, R. K.; Yadav, R. M.; Verma, R. K.; Singh, D. P.; Tan, W. K.; del Pino, A. P.; Moshkalev, S. A. et al. A review on synthesis of graphene, h-BN and MoS_2 for energy storage applications: Recent progress and perspectives. *Nano Res.* **2019**, *12*, 2655–2694.

[9] Lee, C.; Wei, X. D.; Kysar, J. W.; Hone, J. Measurement of the elastic properties and intrinsic strength of monolayer graphene. *Science* **2008**, *321*, 385–388.

[10] Yang, L. S.; Chen, W. J.; Yu, Q. M.; Liu, B. L. Mass production of two-dimensional materials beyond graphene and their applications. *Nano Res*. **2021**, *14*, 1583–1597.

[11] Maqbool, M.; Guo, H. C.; Bashir, A.; Usman, A.; Abid, A. Y.; He, G. S.; Ren, Y. J.; Ali, Z.; Bai, S. L. Enhancing through-plane thermal conductivity of fluoropolymer composite by developing *in situ* nano-urethane linkage at graphene-graphene interface. *Nano Res*. **2020**, *13*, 2741–2748.

[12] Zhang, Y. B.; Tan, Y. W.; Stormer, H. L.; Kim, P. Experimental observation of the quantum Hall effect and Berry's phase in graphene. *Nature* **2005**, *438*, 201–204.

[13] Xue, Y. Z.; Wu, B.; Guo, Y. L.; Huang, L. P.; Jiang, L.; Chen, J. Y.; Geng, D. C.; Liu, Y. Q.; Hu, W. P.; Yu, G. Synthesis of large-area, few-layer graphene on iron foil by chemical vapor deposition. *Nano Res.* **2011**, *4*, 1208–1214.

[14] Yang, X. J.; Yan, M. D. Removing contaminants from transferred CVD graphene. *Nano Res.* **2020**, *13*, 599–610.

[15] Dreyer, D. R.; Park, S. J.; Bielawski, C. W.; Ruoff, R. S. The chemistry of graphene oxide. Chem. Soc. Rev. 2010, 39, 228–240.

[16] Reina, A.; Thiele, S.; Jia, X. T.; Bhaviripudi, S.; Dresselhaus, M. S.; Schaefer, J. A.; Kong, J. Growth of large-area single- and Bi-layer graphene by controlled carbon precipitation on polycrystalline Ni surfaces. *Nano Res*. **2009**, *2*, 509–516.

[17] Wu, Y. P.; Wang, B.; Ma, Y. F.; Huang, Y.; Li, N.; Zhang, F.; Chen, Y. S. Efficient and large-scale synthesis of few-layered graphene using an arc-discharge method and conductivity studies of the resulting films. *Nano Res*. **2010**, *3*, 661–669.

[18] Malik, S.; Vijayaraghavan, A.; Erni, R.; Ariga, K.; Khalakhan, I.; Hill, J. P. High purity graphenes prepared by a chemical intercalation method. *Nanoscale* **2010**, *2*, 2139–2143.

[19] Dai, B. Y.; Fu, L.; Liao, L.; Liu, N.; Yan, K.; Chen, Y. S.; Liu, Z. F. High-quality single-layer graphene via reparative reduction of graphene oxide. *Nano Res*. **2011**, *4*, 434–439.

[20] Hong, Y. Z.; Wang, Z. Y.; Jin, X. B. Sulfuric acid intercalated graphite oxide for graphene preparation. *Sci. Rep*. **2013**, *3*, 3439.

[21] Liu, B. Z.; Wang, H. H.; Gu, W.; Zhou, L.; Chen, Z. L.; Nie, Y. F.; Tan, C. W.; Ci, H. N.; Wei, N.; Cui, L. Z. et al. Oxygen-assisted direct growth of large-domain and high-quality graphene on glass targeting advanced optical filter applications. *Nano Res.* **2020**, *14*, 260–267.

[22] Higginbotham, A. L.; Kosynkin, D. V.; Sinitskii, A.; Sun, Z. Z.; Tour, J. M. Lower-defect graphene oxide nanoribbons from multiwalled carbon nanotubes. *ACS Nano* **2010**, *4*, 2059–2069.

[24] Gurunathan, S.; Han, J. W.; Kim, J. H. Green chemistry approach for the synthesis of biocompatible graphene. *Int. J. Nanomedicine* **2013**, *8*, 2719–2732.

[25] Jiang, B.; Zhao, Q. Y.; Zhang, Z. P.; Liu, B. Z.; Shan, J. Y.; Zhao, L.; Rümmeli, M. K.; Gao, X.; Zhang, Y. F.; Yu, T. J. et al. Batch synthesis of transfer-free graphene with wafer-scale uniformity. *Nano Res.* **2020**, *13*, 1564–1570.

[25] Paredes, J. I.; Villar-Rodil, S.; Fernández-Merino, M. J.; Guardia, L.; Martínez-Alonso, A.; Tascón, J. M. D. Environmentally friendly approaches toward the mass production of processable graphene from graphite oxide. *J. Mater. Chem*. **2011**, *21*, 298–306.

[26] Qian, W.; Hao, R.; Hou, Y. L.; Tian, Y.; Shen, C. M.; Gao, H. J.; Liang, X. L. Solvothermal-assisted exfoliation process to produce graphene with high yield and high quality. *Nano Res.* **2009**, *2*, 706– 712.

[27] Chen, J. P.; Shi, W. L.; Gao, Z. F.; Wang, T.; Wang, S.; Dong, L. J.; Yang, Q. L.; Xiong, C. X. Facile preparation of pristine graphene using urea/glycerol as efficient stripping agents. *Nano Res*. **2018**, *11*, 820–830.

[28] Erythropel, H. C.; Zimmerman, J. B.; de Winter, T. M.; Petitjean, L.; Melnikov, F.; Lam, C. H.; Lounsbury, A. W.; Mellor, K. E.; Janković, N. Z.; Tu, Q. S. et al. The Green ChemisTREE: 20 years after taking root with the 12 principles. *Green Chem.* **2018**, *20*, 1929–1961.

[29] Rogers, L.; Jensen, K. F. Continuous manufacturing – the Green Chemistry promise. *Green Chem.* **2019**, *21*, 3481–3498.

[30] Wang, G. M.; Qian, F.; Saltikov, C. W.; Jiao, Y. Q.; Li, Y. Microbial reduction of graphene oxide by *Shewanella*. *Nano Res*. **2011**, *4*, 563–570.

[31] Sheldon, R. A. The *E* factor 25 years on: The rise of green chemistry and sustainability. *Green Chem*. **2017**, *19*, 18–43.

[32] Iacopi, F.; McIntosh, M. Opportunities and perspectives for green chemistry in semiconductor technologies. *Green Chem*. **2019**, *21*, 3250–3255.

[33] Soldano, C.; Mahmood, A.; Dujardin, E. Production, properties and potential of graphene. *Carbon* **2010**, *48*, 2127–2150.

[34] Yi, M.; Shen, Z. G. A review on mechanical exfoliation for the scalable production of graphene. *J. Mater. Chem. A* **2015**, *3*, 11700–11715.

[35] Alaferdov, A. V.; Gholamipour-Shirazi, A.; Canesqui, M. A.; Danilov, Y. A.; Moshkalev, S. A. Size-controlled synthesis of graphite nanoflakes and multi-layer graphene by liquid phase exfoliation of natural graphite. *Carbon* **2014**, *69*, 525–535.

[36] Cai, M. Z.; Thorpe, D.; Adamson, D. H.; Schniepp, H. C. Methods of graphite exfoliation. *J. Mater. Chem*. **2012**, *22*, 24992–25002.

[37] Fu, Y. X.; Wang, X. M.; Mo, D. C.; Lu, S. S. Production of monolayer, trilayer, and multi-layer graphene sheets by a re-expansion and exfoliation method. *J. Mater. Sci*. **2014**, *49*, 2315–2323.

[38] Guo, S. J.; Dong, S. J. Graphenenanosheet: Synthesis, molecular engineering, thin film, hybrids, and energy and analytical applications. *Chem. Soc. Rev.* **2011**, *40*, 2644–2672.

[39] De Silva, K. K. H.; Huang, H. H.; Joshi, R. K.; Yoshimura, M. Chemical reduction of graphene oxide using green reductants. *Carbon* **2017**, *119*, 190–199.

[40] Chua, C. K.; Pumera, M. Covalent chemistry on graphene. *Chem. Soc. Rev.* **2013**, *42*, 3222–3233.

[41] Choi, S. H.; Lee, J. K.; Kang, Y. C. Three-dimensional porous graphene-metal oxide composite microspheres: Preparation and application in Li-ion batteries. *Nano Res.* **2015**, *8*, 1584–1594.

[42] Chua, C. K.; Sofer, Z.; Pumera, M. Graphite oxides: Effects of permanganate and chlorate oxidants on the oxygen composition. *Chem.—Eur. J.* **2012**, *18*, 13453–13459.

[43] Brodie, B. C. Sur le poids atomique du graphite. *Ann. Chim. Phys*. **1860**, *59*, 466–472.

[44] Staudenmaier, L. Verfahren zur Darstellung der Graphitsäure. *Ber. Dtsch. Chem. Ges*. **1898**, *31*, 1481–1487.

[45] Chua, C. K.; Pumera, M. Chemical reduction of graphene oxide: A synthetic chemistry viewpoint. *Chem. Soc. Rev*. **2014**, *43*, 291–312.

[46] Chua, C. K.; Pumera, M. Reduction of graphene oxide with substituted borohydrides. *J. Mater. Chem. A* **2013**, *1*, 1892–1898.

[47] Pham, V. H.; Hur, S. H.; Kim, E. J.; Kim, B. S.; Chung, J. S. Highly efficient reduction of graphene oxide using ammonia borane. *Chem. Commun*. **2013**, *49*, 6665–6667.

[48] Ambrosi, A.; Chua, C. K.; Bonanni, A.; Pumera, M. Lithium aluminum hydride as reducing agent for chemically reduced graphene oxides. *Chem. Mater*. **2012**, *24*, 2292–2298.

[49] Moon, I. K.; Lee, J. Y.; Ruoff, R. S.; Lee, H. Reduced graphene oxide by chemical graphitization. *Nat. Commun*. **2010**, *1*, 73.

[50] Qi, M.; Song, J. P.; Jin, C.; Li, Z. P.; Liu, J. H.; Meng, S. M.; Zhao, J. G.; Guo, Y. A rapid and easy approach for the reduction of graphene oxide by formamidinesulfinic acid. *Carbon* **2013**, *54*, 36–41.

[51] Pham, V. H.; Cuong, T. V.; Nguyen-Phan, T. D.; Pham, H. D.; Kim, E. J.; Hur, S. H.; Shin, E. W.; Kim, S.; Chung, J. S. One-step synthesis of superior dispersion of chemically converted graphene in organic solvents. *Chem. Commun*. **2010**, *46*, 4375–4377.

[52] Zhang, S.; Shao, Y. Y.; Liao, H. G.; Engelhard, M. H.; Yin, G. P.; Lin, Y. H. Polyelectrolyte-induced reduction of exfoliated graphite oxide: A facile route to synthesis of soluble graphene nanosheets. *ACS Nano* **2011**, *5*, 1785–1791.

[53] Dreyer, D. R.; Murali, S.; Zhu, Y. W.; Ruoff, R. S.; Bielawski, C. W. Reduction of graphite oxide using alcohols. *J. Mater. Chem*. **2011**, *21*, 3443–3447.

[54] Li, J.; Xiao, G. Y.; Chen, C. B.; Li, R.; Yan, D. Y. Superior dispersions of reduced graphene oxide synthesized by using gallic acid as a reductant and stabilizer. *J. Mater. Chem. A* **2013**, *1*, 1481–1487.

[55] Liu, Y. Z.; Li, Y. F.; Yang, Y. G.; Wen, Y. F.; Wang, M. Z. Reduction of graphene oxide by thiourea. *J. Nanosci. Nanotechnol*. **2011**, *11*, 10082–10086.

[56] Some, S.; Kim, Y. M.; Yoon, Y. H.; Yoo, H. J.; Lee, S.; Park, Y.; Lee, H. High-quality reduced graphene oxide by a dual-function chemical reduction and healing process. *Sci. Rep*. **2013**, *3*, 1929.

[57] Pham, V. H.; Pham, H. D.; Dang, T. T.; Hur, S. H.; Kim, E. J.; Kong, B. S.; Kim, S.; Chung, J. S. Chemical reduction of an aqueous suspension of graphene oxide by nascent hydrogen. *J. Mater. Chem*. **2012**, *22*, 10530–10536.

[58] Barman, B. K.; Mahanandia, P.; Nanda, K. K. Instantaneous reduction of graphene oxide at room temperature. *RSC Adv*. **2013**, *3*, 12621–12624.

[59] Liu, Y. S; Luo, F. P. Large-scale highly ordered periodic Au nano-discs/graphene and graphene/Au nanoholes plasmonic substrates for surface-enhanced Raman scattering. *Nano Res*. **2019**, *12*, 2788–2795.

[60] Yang, S.; Yue, W. B.; Huang, D. Z.; Chen, C. F.; Lin, H.; Yang, X. J. A facile green strategy for rapid reduction of graphene oxide by metallic zinc. *RSC Adv*. **2012**, *2*, 8827–8832.

[61] Feng, H. B.; Cheng, R.; Zhao, X.; Duan, X. F.; Li, J. H. A low-temperature method to produce highly reduced graphene oxide. *Nat Commun*. **2013**, *4*, 1539.

[62] Bose, S.; Kuila, T.; Mishra, A. K.; Kim, N. H.; Lee, J. H. Dual role of glycine as a chemical functionalizer and a reducing agent in the preparation of graphene: An environmentally friendly method. *J. Mater. Chem*. **2012**, *22*, 9696–9703.

[63] Ma, J. K.; Wang, X. R.; Liu, Y.; Wu, T.; Liu, Y.; Guo, Y. Q.; Li, R. Q.; Sun, X. Y.; Wu, F.; Li, C. B. et al. Reduction of graphene oxide with L-lysine to prepare reduced graphene oxide stabilized with polysaccharide polyelectrolyte. *J. Mater. Chem. A* **2013**, *1*, 2192–2201.

[64] Thakur, S.; Karak, N. Green reduction of graphene oxide by aqueous phytoextracts. *Carbon* **2012**, *50*, 5331–5339.

[65] Haghighi, B.; Tabrizi, M. A. Green-synthesis of reduced graphene oxide nanosheets using rose water and a survey on their characteristics and applications. *RSC Adv*. **2013**, *3*, 13365–13371.

[66] Kuila, T.; Bose, S.; Khanra, P.; Mishra, A. K.; Kim, N. H.; Lee, J. H. A green approach for the reduction of graphene oxide by wild carrot root. *Carbon* **2012**, *50*, 914–921.

[67] Liu, J. B.; Fu, S. H.; Yuan, B.; Li, Y. L.; Deng, Z. X. Toward a universal “adhesive nanosheet” for the assembly of multiple nanoparticles based on a protein-induced reduction/decoration of graphene oxide. *J. Am. Chem. Soc*. **2010**, *132*, 7279–7281.

[68] Esfandiar, A.; Akhavan, O.; Irajizad, A. Melatonin as a powerful bio-antioxidant for reduction of graphene oxide. *J. Mater. Chem*. **2011**, *21*, 10907–10914.

[69] Somani, P. R.; Somani, S. P.; Umeno, M. Planer nano-graphenes from camphor by CVD. *Chem. Phys. Lett*. **2006**, *430*, 56–59.

[70] Xia, K. L.; Wang, C. Y.; Jian, M. Q.; Wang, Q.; Zhang, Y. Y. CVD growth of fingerprint-like patterned 3D graphene film for an ultrasensitive pressure sensor. *Nano Res*. **2018**, *11*, 1124–1134.

[71] Zhang, Y.; Zhang, L. Y.; Zhou, C. W. Review of chemical vapor deposition of graphene and related applications. *Acc. Chem. Res*. **2013**, *46*, 2329–2339.

[72] Orofeo, C. M.; Ago, H.; Hu, B. S.; Tsuji, M. Synthesis of large area, homogeneous, single layer graphene films by annealing amorphous carbon on Co and Ni. *Nano Res*. **2011**, *4*, 531–540.

[73] Li, X. S.; Cai, W. W.; An, J. H.; Kim, S.; Nah, J.; Yang, D. X.; Piner, R.; Velamakanni, A.; Jung, I.; Tutuc, E. et al. Large-area synthesis of high-quality and uniform graphene films on copper foils. *Science* **2009**, *324*, 1312–1314.

[74] Sutter, P. W.; Flege, J. I.; Sutter, E. A. Epitaxial graphene on ruthenium. *Nat. Mater*. **2008**, *7*, 406–411.

[75] Coraux, J.; N‘Diaye, A. T.; Busse, C.; Michely, T. Structural coherency of graphene on Ir(111). *Nano Lett*. **2008**, *8*, 565–570.

[76] Sutter, P.; Sadowski, J. T.; Sutter, E. Graphene on Pt (111): Growth and substrate interaction. *Phys. Rev. B* **2009**, *80*, 245411.

[77] Varykhalov, A.; Rader, O. Graphene grown on Co (0001) films and islands: Electronic structure and its precise magnetization dependence. *Phys. Rev. B* **2009**, *80*, 035437.

[78] Kwon, S. Y.; Ciobanu, C. V.; Petrova, V.; Shenoy, V. B.; Bareño, J.; Gambin, V.; Petrov, I.; Kodambaka, S. Growth of semiconducting graphene on palladium. *Nano Lett*. **2009**, *9*, 3985–3990.

[79] Miniussi, E.; Pozzo, M.; Baraldi, A.; Vesselli, E.; Zhan, R. R.; Comelli, G.; Menteş, T. O.; Niño, M. A.; Locatelli, A.; Lizzit, S. et al. Thermal stability of corrugated epitaxial graphene grown on Re(0001). *Phys. Rev. Lett*. **2011**, *106*, 216101.

[80] Muñoz, B.; Gómez-Aleixandre, C. Review of CVD synthesis of graphene. *Chem. Vapor Depos*. **2013**, *19*, 297–322.

[81] Lu, C.; Li, Z. Z.; Xia, Z.; Ci, H. N.; Cai, J. S.; Song, Y. Z.; Yu, L. H.; Yin, W. J.; Dou, S. X.; Sun, J. Y. et al. Confining MOF-derived SnSe nanoplatelets in nitrogen-doped graphene cages via direct CVD for durable sodium ion storage. *Nano Res*. **2019**, *12*, 3051–3058.

[82] Kraus, J.; Böcklein, S.; Reichelt, R.; Günther, S.; Santos, B.; Menteş, T. O.; Locatelli, A. Towards the perfect graphene membrane? – Improvement and limits during formation of high quality graphene grown on Cu-foils. *Carbon* **2013**, *64*, 377–390.

[83] Srivastava, A.; Galande, C.; Ci, L. J.; Song, L.; Rai, C.; Jariwala, D.; Kelly, K. F.; Ajayan, P. M. Novel liquid precursor-based facile synthesis of large-area continuous, single, and few-layer graphene films. *Chem. Mater*. **2010**, *22*, 3457–3461.

[84] Zhang, B.; Lee, W. H.; Piner, R.; Kholmanov, I.; Wu, Y. P.; Li, H. F.; Ji, H. X.; Ruoff, R. S. Low-temperature chemical vapor deposition growth of graphene from toluene on electropolished copper foils. *ACS Nano*. **2012**, *6*, 2471–2476.

[85] Huet, B.; Raskin, J. P. Pressure-controlled chemical vapor deposition of single-layer graphene with millimeter-size domains on thin copper film. *Chem. Mater*. **2017**, *29*, 3431–3440.

[86] Huet, B.; Raskin, J. P. Role of Cu foil *in-situ* annealing in controlling the size and thickness of CVD graphene domains. *Carbon* **2018**, *129*, 270–280.

[87] Huet, B.; Raskin, J. P. Role of the Cu substrate in the growth of ultra-flat crack-free highly-crystalline single-layer graphene. *Nanoscale* **2018**, *10*, 21898–21909.

[88] Liu, W.; Li, H.; Xu, C.; Khatami, Y.; Banerjee, K. Synthesis of high-quality monolayer and bilayer graphene on copper using chemical vapor deposition. *Carbon* **2011**, *49*, 4122–4130.

[89] Deokar, G.; Avila, J.; Razado-Colambo, I.; Codron, J. L.; Boyaval, C.; Galopin, E.; Asensio, M. C.; Vignaud, D. Towards high quality CVD graphene growth and transfer. *Carbon* **2015**, *89*, 82–92.

[90] Gao, Y. J.; Chen, X.; Zhang, J. G.; Asakura, H.; Tanaka, T.; Teramura, K.; Ma, D.; Yan, N. Popping of graphite oxide: Application in preparing metal nanoparticle catalysts. *Adv. Mater*. **2015**, *27*, 4688–4694.

[91] Kalita, G.; Masahiro, M.; Uchida, H.; Wakita, K.; Umeno, M. Few layers of graphene as transparent electrode from botanical derivative camphor. *Mater. Lett*. **2010**, *64*, 2180–2183.

[92] Zhang, B. B.; Song, J. L.; Yang, G. Y.; Han, B. X. Large-scale production of high-quality graphene using glucose and ferric chloride. *Chem. Sci*. **2014**, *5*, 4656–4660.

[93] Ruan, G. D.; Sun, Z. Z.; Peng, Z. W.; Tour, J. M. Growth of graphene from food, insects, and waste. *ACS Nano* **2011**, *5*, 7601–7607.

[94] Mouhib, M.; Antonucci, A.; Reggente, M.; Amirjani, A.; Gillen, A. J.; Boghossian, A. A.; Enhancing bioelectricity generation in microbial fuel cells and biophotovoltaics using nanomaterials. *Nano Res*. **2019**, *12*, 2184–2199.

[95] Fredrickson, J. K.; Romine, M. F.; Beliaev, A. S.; Auchtung, J. M.;

Driscoll, M. E.; Gardner, T. S.; Nealson, K. H.; Osterman, A. L.; Pinchuk, G.; Reed, J. L. et al. Towards environmental systems biology of *Shewanella*. *Nat. Rev. Microbiol*. **2008**, *6*, 592–603.

[96] Salas, E. C.; Sun, Z. Z.; Lüttge, A.; Tour, J. M. Reduction of graphene oxide via bacterial respiration. *ACS Nano* **2010**, *4*, 4852–4856.

[97] Zhang, H. M.; Yu, X. Z.; Guo, D.; Qu, B. H.; Zhang, M.; Li, Q. H.; Wang, T. H. Synthesis of bacteria promoted reduced graphene oxide-nickel sulfide networks for advanced supercapacitors. *ACS Appl. Mater. Interfaces* **2013**, *5*, 7335–7340.

[98] Gurunathan, S.; Han, J. W.; Eppakayala, V.; Kim, J. H. Microbial reduction of graphene oxide by *Escherichia coli*: A green chemistry approach. *Colloids Surf B Biointerfaces* **2013**, *102*, 772–777.

[99] Zhu, C. Z.; Guo, S. J.; Fang, Y. X.; Dong, S. J. Reducing sugar: New functional molecules for the green synthesis of graphene nanosheets. *ACS Nano* **2010**, *4*, 2429–2437.

[100] Aunkor, M. T. H.; Mahbubul, I. M.; Saidur, R.; Metselaar, H. S. C. The green reduction of graphene oxide. *RSC Adv*. **2016**, *6*, 27807–27828.

[101] Fernández-Merino, M. J.; Guardia, L.; Paredes, J. I.; Villar-Rodil, S.; Solís-Fernández, P.; Martínez-Alonso, A.; Tascón, J. M. D. Vitamin C is an ideal substitute for hydrazine in the reduction of graphene oxide suspensions. *J. Phys. Chem. C* **2010**, *114*, 6426–6432.

[102] Gao, J.; Liu, F.; Liu, Y. L.; Ma, N.; Wang, Z. Q.; Zhang, X. Environment-friendly method to produce graphene that employs vitamin C and amino acid. *Chem. Mater.* **2010**, *22*, 2213–2218.

[103] Stankovich, S.; Dikin, D. A.; Piner, R. D.; Kohlhaas, K. A.; Kleinhammes, A.; Jia, Y. Y.; Wu, Y.; Nguyen, S. T.; Ruoff, R. S. Synthesis of graphene-based nanosheets via chemical reduction of exfoliated graphite oxide. *Carbon* **2007**, *45*, 1558–1565.

[104] Silberberg, A. Basic principles of colloid science: D. H. Everett, Royal Society of Chemistry, London, 1988. 243 (xv) pp. *J. Colloid Interface Sci*. **1990**, *134*, 593–594.

[105] Li, D.; Müller, M. B.; Gilje, S.; Kaner, R. B.; Wallace, G. G. Processable aqueous dispersions of graphene nanosheets. *Nat. Nanotechnol.* **2008**, *3*, 101–105.

[106] Hunter, R. J. *Foundations of Colloid Science*; Oxford University Press: Oxford, 2001; pp 376−377.

[107] Dukhin, S. S. Dielectric properties of disperse systems. *Surface and colloid science*. 1971, 3, 83–165.

[108] Kashyap, S.; Mishra, S.; Behera, S. K. Aqueous colloidal stability of graphene oxide and chemically converted graphene. *J. Nanopart.* **2014**, *2014*, 640281.

[109] Tian, S. Y.; Yang, S. W.; Huang, T.; Sun, J.; Wang, H. S.; Pu, X. P.; Tian, L. F.; He, P.; Ding, G. Q.; Xie, X. M. One-step fast electrochemical fabrication of water-dispersible graphene. *Carbon* **2017**, *111*, 617–621.

[110] Unalan, I. U.; Wang, C. Y.; Trabattoni, S.; Piergiovanni, L.; Farris, S. Polysaccharide-assisted rapid exfoliation of graphite platelets into high quality water-dispersible graphene sheets. *RSC Adv*. **2015**, *5*, 26482–26490.

[111] Liu, Z. Y.; Zhang, H.; Eredia, M.; Qiu, H. X.; Baaziz, W.; Ersen, O.; Ciesielski, A.; Bonn, M.; Wang, H. I.; Samorì, P. Water-dispersed high-quality graphene: A green solution for efficient energy storage applications. *ACS Nano* **2019**, *13*, 9431–9441.

[112] Bepete, G.; Anglaret, E.; Ortolani, L.; Morandi, V.; Huang, K.; Pénicaud, A.; Drummond, C. Surfactant-free single-layer graphene in water. *Nat. Chem*. **2017**, *9*, 347–352.

[113] Kim, K. S.; Zhao, Y.; Jang, H.; Lee, S. Y.; Kim, J. M.; Kim, K. S.; Ahn, J. H.; Kim, P.; Choi, J. Y.; Hong, B. H. Large-scale pattern growth of graphene films for stretchable transparent electrodes. *Nature* **2009**, *457*, 706–710.

[114] Levendorf, M. P.; Kim, C. J.; Brown, L.; Huang, P. Y.; Havener, R. W.; Muller, D. A.; Park, J. Graphene and boron nitride lateral heterostructures for atomically thin circuitry. *Nature* **2012**, *488*, 627–632.

[115] Nguyen, T. H.; Perilli, D.; Cattelan, M.; Liu, H. S.; Sedona, F.; Fox, N. A.; Di Valentin, C.; Agnoli, S. Microscopic insight into the single step growth of in-plane heterostructures between graphene and hexagonal boron nitride. *Nano Res*. **2019**, *12*, 675–682.

[116] Nair, R. R.; Blake, P.; Grigorenko, A. N.; Novoselov, K. S.; Booth, T. J.; Stauber, T.; Peres, N. M. R.; Geim, A. K. Fine structure constant defines visual transparency of graphene. *Science* **2008**, *320*, 1308.

[117] Han, T. H.; Lee, Y. B.; Choi, M. R.; Woo, S. H.; Bae, S. H.; Hong, B. H.; Ahn, J. H.; Lee, T. W. Extremely efficient flexible organic light-emitting diodes with modified graphene anode. *Nat. Photonics* **2012**, *6*, 105–110.

[118] Son, D. I.; Kwon, B. W.; Park, D. H.; Seo, W. S.; Yi, Y.; Angadi, B.; Lee, C. L.; Choi, W. K. Emissive ZnO–graphene quantum dots for white-light-emitting diodes. *Nat. Nanotechnol*. **2012**, *7*, 465–471.

[119] Zhang, Y.; Wang, J. S.; Qiu, J. J.; Jin, X.; Umair, M. M.; Lu, R. W.; Zhang, S. F.; Tang, B. T. Ag-graphene/PEG composite phase change materials for enhancing solar-thermal energy conversion and storage capacity. *Appl. Energy* **2019**, *237*, 83–90.

[120] Khandelwal, M.; Hur, S. H.; Chung, J. S. Tailoring the structural properties of simultaneously reduced and functionalized graphene oxide via alkanolamine(s)/alkyl alkanolamine for energy storage applications. *Chem. Eng. J*. **2019**, *363*, 120–132.

[121] Ghaly, H. A.; El-Deen, A. G.; Souaya, E. R.; Allam, N. K. Asymmetric supercapacitors based on 3D graphene-wrapped V_2O_5 nanospheres and Fe_3O_4@3D graphene electrodes with high power and energy densities. *Electrochim. Acta* **2019**, *310*, 58–69.

[122] Fang, H.; Meng, F. T.; Yan, J.; Chen, G. Y.; Zhang, L. S.; Wu, S. D.; Zhang, S. C.; Wang, L. Z.; Zhang, Y. X. Fe_3O_4 hard templating to assemble highly wrinkled graphene sheets into hierarchical porous film for compact capacitive energy storage. *RSC Adv*. **2019**, *9*, 20107–20112.

[123] Chen, D. Z.; Qin, S. Y.; Tsui, G. C. P.; Tang, C. Y.; Ouyang, X.; Liu, J. H.; Tang, J. N.; Zuo, J. D. Fabrication, morphology and thermal properties of octadecylamine-grafted graphene oxide-modified phase-change microcapsules for thermal energy storage. *Compos. B: Eng*. **2019**, *157*, 239–247.

[124] Samantara, A. K.; Kamila, S.; Ghosh, A.; Jena, B. K. Highly ordered 1D $NiCo_2O_4$ nanorods on graphene: An efficient dual-functional hybrid materials for electrochemical energy conversion and storage applications. *Electrochim. Acta* **2018**, *263*, 147–157.

[125] Liu, X. X.; Chao, D. L.; Su, D. P.; Liu, S. K.; Chen, L.; Chi, C. X.; Lin, J. Y.; Shen, Z. X.; Zhao, J. P.; Mai, L. Q. et al. Graphene nanowires anchored to 3D graphene foam via self-assembly for high performance Li and Na ion storage. *Nano Energy* **2017**, *37*, 108–117.

[126] Deshmukh, K.; Ahamed, M. B.; Deshmukh, R. R.; Pasha, S. K. K.; Sadasivuni, K. K.; Ponnamma, D.; Chidambaram, K. Synergistic effect of vanadium pentoxide and graphene oxide in polyvinyl alcohol for energy storage application. *Eur. Polym. J*. **2016**, *76*, 14–27.

[127] Amin, M.; Putra, N.; Kosasih, E. A.; Prawiro, E.; Mahlia, T. M. I. Thermal properties of beeswax/graphene phase change material as energy storage for building applications. *Appl. Therm. Eng*. **2017**, *112*, 273–280.

[128] Vineesh, T. V.; Mubarak, S.; Hahm, M. G.; Prabu, V.; Alwarappan, S.; Narayanan, T. N. Controllably alloyed, low density, free-standing Ni-Co and Ni-graphene sponges for electrocatalytic water splitting. *Sci. Rep*. **2016**, *6*, 31202.

[129] Zhang, B.; Sun, G.; Ding, S. P.; Asakura, H.; Zhang, J.; Sautet, P.; Yan, N. Atomically dispersed Pt_1–polyoxometalate catalysts: How does metal–support interaction affect stability and hydrogenation activity. *J. Am. Chem. Soc*. **2019**, *141*, 8185–8197.

[130] Sahraei, R.; Pour, Z. S.; Ghaemy, M. Novel magnetic bio-sorbent hydrogel beads based on modified gum tragacanth/graphene oxide: Removal of heavy metals and dyes from water. *J. Clean. Prod*. **2017**, *142*, 2973–2984.

[131] Li, J.; Zhang, D. Z.; Yang, T. T.; Yang, S.; Yang, X. D.; Zhu, H. W. Nanofibrous membrane of graphene oxide-in-polyacrylonitrile composite with low filtration resistance for the effective capture of $PM_{2.5}$. *J. Memb. Sci*. **2018**, *551*, 85–92.

[132] Singh, S. B.; Hussain, C. M. Nano-graphene as groundbreaking miracle material: Catalytic and commercial perspectives. *ChemistrySelect* **2018**, *3*, 9533–9544.

[133] Su, Y.; Zhang, Y. F.; Qi, J. X.; Xue, T. T.; Xu, M. G.; Yang, J. Z.; Pan, Y.; Lin, Z. K. Upgrading of furans from *in situ* catalytic

fast pyrolysis of xylan by reduced graphene oxide supported Pt nanoparticles. *Renew. Energy* **2020**, *152*, 94–101.

[134] Lan, Y. F.; Li, X. Y.; Li, G. P.; Luo, Y. J. Sol–gel method to prepare graphene/Fe_2O_3 aerogel and its catalytic application for the thermal decomposition of ammonium perchlorate. *J. Nanopart. Res*. **2015**, *17*, 395.

[135] Hong, W.; Li, L. J.; Xue, Y. N.; Xu, X. Y.; Wang, H.; Zhou, J. K.; Zhao, H. L.; Song, Y. H.; Liu, Y.; Gao, J. P. One-pot hydrothermal synthesis of zinc ferrite/reduced graphene oxide as an efficient electrocatalyst for oxygen reduction reaction. *J. Colloid. Interface. Sci*. **2017**, *485*, 175–182.

[136] Zu, Y. Q.; Zhang, Y.; Xu, K. Z.; Zhao, F. Q. A graphene oxide–$MgWO_4$ nanocomposite as an efficient catalyst for the thermal decomposition of RDX, HMX. *RSC Adv*. **2016**, *6*, 31046–31052.

[137] Liu, B.; Wang, W. M.; Wang, J. J.; Zhang, Y.; Xu, K. Z.; Zhao, F. Q. Preparation and catalytic activities of $CuFe_2O_4$ nanoparticles assembled with graphene oxide for RDX thermal decomposition. *J. Nanopart. Res*. **2019**, *21*, 48.

[138] Chen, J.; Xiao, P.; Gu, J. C.; Huang, Y. J.; Zhang, J. W.; Wang, W. Q.; Chen, T. Au nanoparticle-loaded PDMAEMA brush grafted graphene oxide hybrid systems for thermally smart catalysis. *RSC Adv*. **2014**, *4*, 44480–44485.

[139] Ali, A. A.; Madkour, M.; Al Sagheer, F.; Zaki, M. I.; Nazeer, A. A. Low-temperature catalytic CO oxidation over non-noble, efficient chromia in reduced graphene oxide and graphene oxide nanocomposites. *Catalysts* **2020**, *10*, 105.

[140] Huang, F.; Deng, Y. C.; Chen, Y. L.; Cai, X. B.; Peng, M.; Jia, Z. M.; Xie, J. L.; Xiao, D. Q.; Wen, X. D.; Wang, N. et al. Anchoring Cu_1 species over nanodiamond-graphene for semi-hydrogenation of acetylene. *Nat. Commun*. **2019**, *10*, 4431.

[141] Zhang, J. Y.; Deng, Y. C.; Cai, X. B.; Chen, Y. L.; Peng, M.; Jia, Z. M.; Jiang, Z.; Ren, P. J.; Yao, S. Y.; Xie, J. L. et al. Tin-assisted fully exposed platinum clusters stabilized on defect-rich graphene for dehydrogenation reaction. *ACS Catal*. **2019**, *9*, 5998–6005.

[142] Karimi, A.; Sadighi, S. Graphene supported NiMo catalyst: A promising novel hydrocracking catalyst. *Int. J. Chem. Kinet*. **2020**, *52*, 378–386.

[143] Liu, J. W.; Ma, Q. L.; Huang, Z. Q.; Liu, G. G.; Zhang, H. Recent progress in graphene-based noble-metal nanocomposites for electrocatalytic applications. *Adv. Mater*. **2019**, *31*, 1800696.

[144] Fan, X. B.; Zhang, G. L.; Zhang, F. B. Multiple roles of graphene in heterogeneous catalysis. *Chem. Soc. Rev*. **2015**, *44*, 3023–3035.

[145] Ta, H. Q.; Zhao, L.; Yin, W. J.; Pohl, D.; Rellinghaus, B.; Gemming, T.; Trzebicka, B.; Palisaitis, J.; Jing, G.; Persson, P. O. Å. et al. Single Cr atom catalytic growth of graphene. *Nano Res*. **2018**, *11*, 2405–2411.

[146] Qiao, B. T.; Wang, A. Q.; Yang, X. F.; Allard, L. F.; Jiang, Z.; Cui, Y. T.; Liu, J. Y.; Li, J.; Zhang, T. Single-atom catalysis of CO oxidation using Pt_1FeO_x. *Nat. Chem*. **2011**, *3*, 634–641.

[147] Fei, H. L.; Dong, J. C.; Chen, D. L.; Hu, T. D.; Duan, X. D.; Shakir, I.; Huang, Y.; Duan, X. F. Single atom electrocatalysts supported on graphene or graphene-like carbons. *Chem. Soc. Rev*. **2019**, *48*, 5207–5241.

[148] Yu, X. M.; Han, P.; Wei, Z. X.; Huang, L. S.; Gu, Z. X.; Peng, S. J.; Ma, J. M.; Zheng, G. F. Boron-doped graphene for electrocatalytic N_2 reduction. *Joule* **2018**, *2*, 1610–1622.

[149] Niu, H. J.; Zhang, L.; Feng, J. J.; Zhang, Q. L.; Huang, H.; Wang, A. J. Graphene-encapsulated cobalt nanoparticles embedded in porous nitrogen-doped graphitic carbon nanosheets as efficient electrocatalysts for oxygen reduction reaction. *J. Colloid Interface Sci*. **2019**, *552*, 744–751.

[150] Yan, J.; Fan, Z. J.; Wei, T.; Qian, W. Z.; Zhang, M. L.; Wei, F. Fast and reversible surface redox reaction of graphene–MnO_2 composites as supercapacitor electrodes. *Carbon* **2010**, *48*, 3825–3833.

[151] Gao, Z. Y.; Liu, X.; Chang, J. L.; Wu, D. P.; Xu, F.; Zhang, L. C.; Du, W. M.; Jiang, K. Graphene incorporated, N doped activated carbon as catalytic electrode in redox active electrolyte mediated supercapacitor. *J. Power Sources* **2017**, *337*, 25–35.

[152] Jafri, R. I.; Rajalakshmi, N.; Ramaprabhu, S. Nitrogen doped graphene nanoplatelets as catalyst support for oxygen reduction reaction in proton exchange membrane fuel cell. *J. Mater. Chem*. **2010**, *20*, 7114–7117.

[153] Ding, S. P.; Hülsey, M. J.; Pérez-Ramírez, J.; Yan, N. Transforming energy with single-atom catalysts. *Joule* **2019**, *3*, 2897–2929.

[154] Li, X. G.; Bi, W. T.; Chen, M. L.; Sun, Y. X.; Ju, H. X.; Yan, W. S.; Zhu, J. F.; Wu, X. J.; Chu, W. S.; Wu, C. Z. et al. Exclusive Ni–N_4 sites realize near-unity CO selectivity for electrochemical CO_2 reduction. *J. Am. Chem. Soc*. **2017**, *139*, 14889–14892.

[155] Hülsey, M. J.; Lim, C. W.; Yan, N. Promoting heterogeneous catalysis beyond catalyst design. *Chem. Sci*. **2020**, *11*, 1456–1468.

[156] Ding, S. P.; Guo, Y. L.; Max J. H.; Zhang, B.; Asakura, H.; Liu, L. M.; Han, Y.; Gao, M.; Hasegawa, J. Y.; Qiao, B. T. et al. Electrostatic stabilization of single-atom catalysts by ionic liquids. *Chem* **2019**, *5*, 3207−3219.

[157] Akira, F.; Kenichi, H. Electrochemical photolysis of water at a semiconductor electrode. *Nature* **1972**, *238*, 37–38.

[158] Williams, G.; Seger, B.; Kamat, P. V. TiO_2-graphene nanocomposites. UV-assisted photocatalytic reduction of graphene oxide. *ACS Nano* **2008**, *2*, 1487–1491.

[159] Li, X.; Yu, J. G.; Wageh, S.; Al-Ghamdi, A. A.; Xie, J. Graphene in photocatalysis: A review. *Small* **2016**, *12*, 6640–6696.

[160] Bie, C. B.; Zhu, B. C.; Xu, F. Y.; Zhang, L. Y.; Yu, J. G. *In situ* grown monolayer N-doped graphene on CdS hollow spheres with seamless contact for photocatalytic CO_2 reduction. *Adv. Mater*. **2019**, *31*, 1902868.

[161] Xu, Y. F.; Yang, M. Z.; Chen, B. X.; Wang, X. D.; Chen, H. Y.; Kuang, D. B.; Su, C. Y. A $CsPbBr_3$ perovskite quantum dot/graphene oxide composite for photocatalytic CO_2 reduction. *J. Am. Chem. Soc*. **2017**, *139*, 5660–5663.

[162] Wang, L.; Li, Z.; Chen, J.; Huang, Y. N.; Zhang, H. J.; Qiu, H. D. Enhanced photocatalytic degradation of methyl orange by porous graphene/ZnO nanocomposite. *Environ. Pollut.* **2019**, *249*, 801–811.

[163] Kuang, Y.; Shang, J.; Zhu, T. Photoactivated graphene oxide to enhance photocatalytic reduction of CO_2. *ACS Appl. Mater. Interfaces* **2020**, *12*, 3580–3591.

[164] Jiang, J. X.; Zhang, Q. Q.; Li, Y. H.; Li, L. Three-dimensional network graphene aerogel for enhancing adsorption and visible light photocatalysis of nitrogen-doped TiO_2. *Mater. Lett*. **2019**, *234*, 298–301.

[165] Dong, S. Y.; Cui, L. F.; Liu, C. Y.; Zhang, F. Y.; Li, K. Y.; Xia, L. J.; Su, X. F.; Feng, J. L.; Zhu, Y. F.; Sun, J. H. Fabrication of 3D ultra-light graphene aerogel/Bi_2WO_6 composite with excellent photocatalytic performance: A promising photocatalysts for water purification. *J. Taiwan Inst. Chem. Eng*. **2019**, *97*, 288–296.

[166] Zhang, H. J.; Xu, P. P.; Du, G. D.; Chen, Z. W.; Oh, K.; Pan, D. Y.; Jiao, Z. A facile one-step synthesis of TiO_2/graphene composites for photodegradation of methyl orange. *Nano Res*. **2011**, *4*, 274–283.

[167] Yu, Q.; Lin, R.; Jiang, L. Y.; Wan, J. W.; Chen, C. Fabrication and photocatalysis of ZnO nanotubes on transparent conductive graphene-based flexible substrates. *Sci. China Mater*. **2018**, *61*, 1007–1011.

[168] McCreery, R. L. Advanced carbon electrode materials for molecular electrochemistry. *Chem. Rev*. **2008**, *108*, 2646–2687.

[169] Jia, J. B.; Kato, D.; Kurita, R.; Sato, Y.; Maruyama, K.; Suzuki, K.; Hirono, S.; Ando, T.; Niwa, O. Structure and electrochemical properties of carbon films prepared by a electron cyclotron resonance sputtering method. *Anal. Chem*. **2007**, *79*, 98–105.

[170] Pumera, M. ChemInform abstract: Graphene-based nanomaterials and their electrochemistry. *Chem. Soc. Rev.* **2010,** 39, 4146–4157.

[171] Lou, Z.; Chen, S.; Wang, L. L.; Jiang, K.; Shen, G. Z. An ultra-sensitive and rapid response speed graphene pressure sensors for electronic skin and health monitoring. *Nano Energy* **2016**, *23*, 7–14.

[172] Huang, L.; Huang, Y.; Liang, J. J.; Wan, X. J.; Chen, Y. S. Graphene-based conducting inks for direct inkjet printing of flexible conductive patterns and their applications in electric circuits and chemical sensors. *Nano Res*. **2011**, *4*, 675–684.

[173] Mansouri, N.; Babadi, A. A.; Bagheri, S.; Hamid, S. B. A. H. Immobilization of glucose oxidase on 3D graphene thin film: Novel glucose bioanalytical sensing platform. *Int. J. Hydrogen Energy* **2017**, *42*, 1337–1343.

[174] Shang, N. G.; Papakonstantinou, P.; McMullan, M.; Chu, M.; Stamboulis, A.; Potenza, A.; Dhesi, S. S.; Marchetto, H. Catalyst-free efficient growth, orientation and biosensing properties of multilayer

graphene nanoflake films with sharp edge planes. *Adv. Funct. Mater*. **2008**, *18*, 3506–3514.

[175] Goryacheva, O. A.; Vostrikova, A. M.; Kokorina, A. A.; Mordovina, E. A.; Tsyupka, D. V.; Bakal, A. A.; Markin, A. V.; Shandilya, R.; Mishra, P. K.; Beloglazova, N. V. et al. Luminescent carbon nanostructures for microRNA detection. *TrAC Trends Anal. Chem*. **2019**, *119*, 115613.

[176] Hébert, C.; Masvidal-Codina, E.; Suarez-Perez, A.; Calia, A. B.; Piret, G.; Garcia-Cortadella, R.; Illa, X.; Del Corro Garcia, E.; De la Cruz Sanchez, J. M.; Casals, D. V. et al. Flexible graphene solution-gated field-effect transistors: Efficient transducers for micro-electrocorticography. *Adv. Funct. Mater*. **2018**, *28*, 1703976.

[177] Kanai, Y.; Ohmuro-Matsuyama, Y.; Tanioku, M.; Ushiba, S.; Ono, T.; Inoue, K.; Kitaguchi, T.; Kimura, M.; Ueda, H.; Matsumoto, K. Graphene field effect transistor-based immunosensor for ultrasensitive noncompetitive detection of small antigens. *ACS Sens*. **2020**, *5*, 24–28.

[178] Shao, Y. Y.; Yin, G. P.; Gao, Y. Z. Understanding and approaches for the durability issues of Pt-based catalysts for PEM fuel cell. *J. Power Sources* **2007**, *171*, 558–566.

[179] Wu, Z. S.; Wang, D. W.; Ren, W. C.; Zhao, J. P.; Zhou, G. M.; Li, F.; Cheng, H. M. Anchoring hydrous RuO_2 on graphene sheets for high-performance electrochemical capacitors. *Adv. Funct. Mater*. **2010**, *20*, 3595–3602.

[180] Dong, L. F.; Gari, R. R. S.; Li, Z.; Craig, M. M.; Hou, S. F. Graphene-supported platinum and platinum–ruthenium nanoparticles with high electrocatalytic activity for methanol and ethanol oxidation. *Carbon* **2010**, *48*, 781–787.

[181] Li, W. Z.; Liang, C. H.; Zhou, W. J.; Qiu, J. S.; Zhou, Z. H.; Sun, G. Q.; Xin, Q. Preparation and characterization of multiwalled carbon nanotube-supported platinum for cathode catalysts of direct methanol fuel cells. *J. Phys. Chem. B* **2003**, *107*, 6292–6299.

[182] Gong, K. P.; Du, F.; Xia, Z. H.; Durstock, M.; Dai, L. M. Nitrogen-doped carbon nanotube arrays with high electrocatalytic activity for oxygen reduction. *Science* **2009**, *323*, 760–764.

[183] Koo, B.; Lee, S. M.; Oh, S. E.; Kim, E. J.; Hwang, Y.; Seo, D.; Kim, J. Y.; Khang, Y. H.; Lee, Y. W.; Chung, S. Y. et al. Addition of reduced graphene oxide to an activated-carbon cathode increases electrical power generation of a microbial fuel cell by enhancing cathodic performance. *Electrochim. Acta* **2019**, *297*, 613–622.

[184] Luo, Z. Y.; Gong, Y. J.; Liao, X. F.; Pana, Y. J.; Zhang, H. W. Nanocomposite membranes modified by graphene-based materials for anion exchange membrane fuel cells. *RSC Adv*. **2016**, *6*, 13618–13625.

[185] Papiya, F.; Das, S.; Pattanayak, P.; Kundu, P. P. The fabrication of silane modified graphene oxide supported Ni–Co bimetallic electrocatalysts: A catalytic system for superior oxygen reduction in microbial fuel cells. *Int. J. Hydrogen Energy* **2019**, *44*, 25874–25893.

[186] Pothaya, S.; Regalbuto, J. R.; Monnier, J. R.; Punyawudho, K. Preparation of Pt/graphene catalysts for polymer electrolyte membrane fuel cells by strong electrostatic adsorption technique. *Int. J. Hydrogen Energy* **2019**, *44*, 26361–26372.

[187] Qu, L. T.; Liu, Y.; Baek, J. B.; Dai, L. M. Nitrogen-doped graphene as efficient metal-free electrocatalyst for oxygen reduction in fuel cells. *ACS Nano* **2010**, *4*, 1321–1326.

[188] Yang, Y.; Xue, Y. S.; Zhang, H.; Chang, H. L. Flexible H_2O_2 microfluidic fuel cell using graphene/Prussian blue catalyst for high performance. *Chem. Eng. J*. **2019**, *369*, 813–817.

[189] Yang, H. J.; Geng, L.; Zhang, Y. T.; Chang, G.; Zhang, Z. L.; Liu, X.; Lei, M.; He, Y. B. Graphene-templated synthesis of palladium nanoplates as novel electrocatalyst for direct methanol fuel cell. *Appl. Surf. Sci*. **2019**, *466*, 385–392.

[190] Yousef, A.; El-Newehy, M. H.; Al-Deyab, S. S.; Barakat, N. A. M. Facile synthesis of Ni-decorated multi-layers graphene sheets as effective anode for direct urea fuel cells. *Arab. J. Chem*. **2017**, *10*, 811–822.

[191] Cheng, Y.; He, S.; Lu, S. F.; Veder, J. P.; Johannessen, B.; Thomsen, L.; Saunders, M.; Becker, T.; De Marco, R.; Li, Q. F. et al. Iron single atoms on graphene as nonprecious metal catalysts for high-temperature polymer electrolyte membrane fuel cells. *Adv. Sci*. **2019**, *6*, 1802066.

[192] Hou, J. B.; Shao, Y. Y.; Ellis, M. W.; Moore, R. B.; Yi, B. L. Graphene-based electrochemical energy conversion and storage: Fuel cells, supercapacitors and lithium ion batteries. *Phys. Chem. Chem. Phys*. **2011**, *13*, 15384–15402.

[193] Tan, Y. B.; Lee, J. M. Graphene for supercapacitor applications. *J. Mater. Chem. A* **2013**, ***1***, 14814–14843.

[194] Shi, W. H.; Zhu, J. X.; Sim, D. H.; Tay, Y. Y.; Lu, Z. Y.; Zhang, X. J.; Sharma, Y.; Srinivasan, M.; Zhang, H.; Hng, H. H. et al. Achieving high specific charge capacitances in Fe_3O_4/reduced graphene oxide nanocomposites. *J. Mater. Chem*. **2011**, *21*, 3422–3427.

[195] Ma, Y. Y.; Yuan, W. Y.; Bai, Y. H.; Wu, H.; Cheng, L. F. The toughening design of pseudocapacitive materials via graphene quantum dots: Towards enhanced cycling stability for supercapacitors. *Carbon* **2019**, *154*, 292–300.

[196] Ramadan, A.; Anas, M.; Ebrahim, S.; Soliman, M.; Abou-Aly A. Effect of co-doped graphene quantum dots to polyaniline ratio on performance of supercapacitor. *J. Mater. Sci.: Mater. Electron*. **2020**, *31*, 7247–7259.

[197] Lei, Z. B.; Zhang, J. T.; Zhao, X. S. Ultrathin MnO_2 nanofibers grown on graphitic carbon spheres as high-performance asymmetric supercapacitor electrodes. *J. Mater. Chem*. **2012**, *22*, 153–160.

[198] Zhang, W. Y.; Yang, Y. N.; Xia, R. Q.; Li, Y. C.; Zhao, J. Q.; Lin, L.; Cao, J. M.; Wang, Q. H.; Liu, Y.; Guo, H. W. Graphene-quantum-dots-induced MnO_2 with needle-like nanostructure grown on carbonized wood as advanced electrode for supercapacitors. *Carbon* **2020**, *162*, 114–123.

[199] Yu, Z. N.; Tetard, L.; Zhai, L.; Thomas, J. Supercapacitor electrode materials: Nanostructures from 0 to 3 dimensions. *Energy Environ. Sci*. **2015**, *8*, 702–730.

[200] Moitra, D.; Anand, C.; Ghosh, B. K.; Chandel, M.; Ghosh, N. N. One-dimensional $BiFeO_3$ nanowire-reduced graphene oxide nanocomposite as excellent supercapacitor electrode material. *ACS Appl. Energy Mater*. **2018**, *1*, 464–474.

[201] Kou, L.; Huang, T. Q.; Zheng, B. N.; Han, Y.; Zhao, X. L.; Gopalsamy, K.; Sun, H. Y.; Gao, C. Coaxial wet-spun yarn supercapacitors for high-energy density and safe wearable electronics. *Nat. Commun*. **2014**, *5*, 3754.

[202] Zhang, G. X.; Xiao, X.; Li, B.; Gu, P.; Xue, H. G.; Pang, H. Transition metal oxides with one-dimensional/one-dimensional-analogue nanostructures for advanced supercapacitors. *J. Mater. Chem. A* **2017**, *5*, 8155–8186.

[203] Lei, Z. B.; Shi, F. H.; Lu, L. Incorporation of MnO_2-coated carbon nanotubes between graphene sheets as supercapacitor electrode. *ACS Appl. Mater. Interfaces* **2012**, *4*, 1058–1064.

[204] Li, Z. M.; An, Y. F.; Hu, Z. G.; An, N.; Zhang, Y. D.; Guo, B. S.; Zhang, Z. Y.; Yang, Y. Y.; Wu, H. Y. Preparation of a two-dimensional flexible MnO_2/graphene thin film and its application in a supercapacitor. *J. Mater. Chem. A* **2016**, *4*, 10618–10626.

[205] Tu, C. C.; Lin, L. Y.; Xiao, B. C.; Chen, Y. S. Highly efficient supercapacitor electrode with two-dimensional tungsten disulfide and reduced graphene oxide hybrid nanosheets. *J. Power Sources* **2016**, *320*, 78–85.

[206] Lee, J. W.; Hall, A. S.; Kim, J. D.; Mallouk, T. E. A facile and template-free hydrothermal synthesis of Mn_3O_4 nanorods on graphene sheets for supercapacitor electrodes with long cycle stability. *Chem. Mater*. **2012**, *24*, 1158–1164.

[207] Yang, J.; Zhang, Y.; Sun, C. C.; Liu, H. Z.; Li, L. Q.; Si, W. L.; Huang, W.; Yan Q. Y.; Dong, X. C. Graphene and cobalt phosphide nanowire composite as an anode material for high performance lithium-ion batteries. *Nano Res*. **2016**, *9*, 612–621.

[208] Xia, X. H.; Tu, J. P.; Mai, Y. J.; Chen, R.; Wang, X. L.; Gu, C. D.; Zhao, X. B. Graphene sheet/porous NiO hybrid film for supercapacitor applications. *Chemistry* **2011**, *17*, 10898–10905.

[209] Chen, Z.; Lu, J. F.; Ai, Y. J.; Ji, Y. F.; Adschiri, T.; Wan, L. J. Ruthenium/graphene-like layered carbon composite as an efficient hydrogen evolution reaction electrocatalyst. *ACS Appl. Mater. Interfaces* **2016**, *8*, 35132–35137.

[210] Xiang, C. C.; Li, M.; Zhi, M. J.; Manivannan, A.; Wu, N. Q. Reduced graphene oxide/titanium dioxide composites for supercapacitor electrodes: Shape and coupling effects. *J. Mater. Chem*. **2012**, *22*, 19161–19167.

[211] Zhu, Q. X.; Qin, F. F.; Lu, J. F.; Zhu, Z.; Nan, H. Y.; Shi, Z. L.; Ni,

Z. H.; Xu, C. X. Synergistic graphene/aluminum surface plasmon coupling for zinc oxide lasing improvement. *Nano Res*. **2017**, *10*, 1996–2004.

[212] Qiu, L.; Yang, X. W.; Gou, X. L.; Yang, W. R.; Ma, Z. F.; Wallace, G. G.; Li, D. Dispersing carbon nanotubes with graphene oxide in water and synergistic effects between graphene derivatives. *Chem.—Eur. J*. **2010**, *16*, 10653–10658.

[213] Yang, X. W.; Zhu, J. W.; Qiu, L.; Li, D. Graphene assembly: Bioinspired effective prevention of restacking in multilayered graphene films: Towards the next generation of high-performance supercapacitors (Adv. Mater. 25/2011). *Adv. Mater*. **2011**, *23*, 2771.

[214] Yang, W. L.; Gao, Z.; Wang, J.; Wang, B.; Liu, Q.; Li, Z. S.; Mann, T.; Yang, P. P.; Zhang, M. L.; Liu, L. H. Synthesis of reduced graphene nanosheet/urchin-like manganese dioxide composite and high performance as supercapacitor electrode. *Electrochim. Acta* **2012**, *69*, 112–119.

[215] Wu, Y. P.; Zhu, J. H.; Huang, L. A review of three-dimensional graphene-based materials: Synthesis and applications to energy conversion/storage and environment. *Carbon* **2019**, *143*, 610–640.

[216] Cao, X. H.; Yin, Z. Y.; Zhang, H. Three-dimensional graphene materials: Preparation, structures and application in supercapacitors. *Energy Environ. Sci*. **2014**, *7*, 1850–1865.

[217] Shah, S. A.; Kulhanek, D.; Sun, W. M.; Zhao, X. F.; Yu, S.; Parviz, D.; Lutkenhaus, J. L.; Green, M. J. Aramid nanofiber-reinforced three-dimensional graphene hydrogels for supercapacitor electrodes. *J. Colloid Interface Sci*. **2020**, *560*, 581–588.

[218] Zhou, R.; Han, C. J.; Wang, X. M. Hierarchical MoS_2-coated three-dimensional graphene network for enhanced supercapacitor performances. *J. Power Sources* **2017**, *352*, 99–110.

[219] Li, S. M.; Yang, K.; Ya, P. W.; Ma, K. R.; Zhang, Z.; Huang, Q. Three-dimensional porous carbon/Co_3O_4 composites derived from graphene/Co-MOF for high performance supercapacitor electrodes. *Appl. Surf. Sci*. **2020**, *503*, 144090.

[220] Ramadoss, A.; Yoon, K. Y.; Kwak, M. J.; Kim, S. I.; Ryu, S. T.; Jang, J. H. Fully flexible, lightweight, high performance all-solid-state supercapacitor based on 3-dimensional-graphene/graphite-paper. *J. Power Sources* **2017**, *337*, 159–165.

[221] He, Y. M.; Chen, W. J.; Li, X. D.; Zhang, Z. X.; Fu, J. C.; Zhao, C. H.; Xie, E. Q. Freestanding three-dimensional graphene/MnO_2 composite networks as ultralight and flexible supercapacitor electrodes. *ACS Nano* **2013**, *7*, 174–182.

[222] Chen, P.; Yang, J. J.; Li, S. S.; Wang, Z.; Xiao, T. Y.; Qian, Y. H.; Yu, S. H. Hydrothermal synthesis of macroscopic nitrogen-doped graphene hydrogels for ultrafast supercapacitor. *Nano Energy* **2013**, *2*, 249–256.

[223] Wang, D. W.; Li, F.; Liu, M.; Lu, G. Q.; Cheng, H. M. 3D aperiodic hierarchical porous graphitic carbon material for high-rate electrochemical capacitive energy storage. *Angew. Chem., Int. Ed*. **2008**, *47*, 373–376.

[224] Chen, Y.; Wang, L. Z.; Shi, J. L. Two-dimensional non-carbonaceous materials-enabled efficient photothermal cancer therapy. *Nano Today* **2016**, *11*, 292–308.

[225] Ghawanmeh, A. A.; Ali, G. A. M.; Algarni, H.; Sarkar, S. M.; Cong, K. F. Graphene oxide-based hydrogels as a nanocarrier for anticancer drug delivery. *Nano Res*. **2019**, *12*, 973–990.

[226] Kiew, S. F.; Ho, Y. T.; Kiew, L. V.; Kah, J. C. Y.; Lee, H. B.; Imae, T.; Chung, L. Y. Preparation and characterization of an amylase-triggered dextrin-linked graphene oxide anticancer drug nanocarrier and its vascular permeability. *Int. J. Pharm*. **2017**, *534*, 297–307.

[227] Liu, Z.; Robinson, J. T.; Sun, X. M.; Dai, H. J. PEGylated nanographene oxide for delivery of water-insoluble cancer drugs. *J. Am. Chem. Soc*. **2008**, *130*, 10876–10877.

[228] Shang, W. H.; Zhang, X. Y.; Zhang, M.; Fan, Z. T.; Sun, Y.; Han, M.; Fan, L. Z. The uptake mechanism and biocompatibility of graphene quantum dots with human neural stem cells. *Nanoscale* **2014**, *6*, 5799–5806.

[229] Xie, M.; Zhang, F.; Liu, L. J.; Zhang, Y. N.; Li, Y. P.; Li, H. M.; Xie, J. M. Surface modification of graphene oxide nanosheets by protamine sulfate/sodium alginate for anti-cancer drug delivery application. *Appl. Surf. Sci*. **2018**, *440*, 853–860.

[230] Gai, L. X.; Wang, W. Q.; Wu, X.; Su, X. J.; Yang, F. C. NIR absorbing reduced graphene oxide for photothermal radiotherapy for treatment of esophageal cancer. *J. Photochem. Photobiol. B* **2019**, *194*, 188–193.

[231] Geng, H.; Qiu, J. J.; Zhu, H. Q.; Liu, X. Y. Achieving stem cell imaging and osteogenic differentiation by using nitrogen doped graphene quantum dots. *J. Mater. Sci*. **2018**, *29*, 85.

[232] Guo, L. L.; Shi, H. L.; Wu, H. X.; Zhang, Y. X.; Wang, X.; Wu, D. M.; Lu A.; Yang, S. P. Prostate cancer targeted multifunctionalized graphene oxide for magnetic resonance imaging and drug delivery. *Carbon* **2016**, *107*, 87–99.

[233] Lima-Sousa, R.; Melo-Diogo, D.; Alves, C. G.; Costa, E. C.; Ferreira, P.; Louro, R. O.; Correia, I. J. Hyaluronic acid functionalized green reduced graphene oxide for targeted cancer photothermal therapy. *Carbohydr. Polym*. **2018**, *200*, 93–99.

[234] Wang, Y.; Zhang, P.; Liu, C. F.; Zhan, L.; Lia, Y. F.; Huang, C. Z. Green and easy synthesis of biocompatible graphene for use as an anticoagulant. *RSC Adv*. **2012**, *2*, 2322–2328.

[235] Sun, X. M.; Liu, Z.; Welsher, K.; Robinson, J. T.; Goodwin, A.; Zaric, S.; Dai, H. J. Nano-graphene oxide for cellular imaging and drug delivery. *Nano Res*. **2008**, *1*, 203–212.

[236] Muñoz, J.; Riba-Moliner, M.; Brennan, L. J.; Gun'ko, Y. K.; Céspedes, F.; González-Campo, A.; Baeza, M. Amperometric thyroxine sensor using a nanocomposite based on graphene modified with gold nanoparticles carrying a thiolated β-cyclodextrin. *Microchim. Acta* **2016**, *183*, 1579–1589.

[237] Yu, Y.; Chen, X.; Yao, Q. F.; Yu, Y.; Yan, N.; Xie, J. P. Scalable and precise synthesis of thiolated $Au_{10–12}$, Au_{15}, Au_{18}, and Au_{25} nanoclusters via pH controlled CO reduction. *Chem. Mater*. **2013**, *25*, 946–952.

[238] Chen, L. Q.; Hu, P. P.; Zhang, L.; Huang, S. Z.; Luo, L. F.; Huang, C. Z. Toxicity of graphene oxide and multi-walled carbon nanotubes against human cells and zebrafish. *Sci. China Chem*. **2012**, *55*, 2209–2216.